AN IUE'S EYE VIEW OF COOL-STAR OUTER ATMOSPHERES

Tom Ayres†
Joint Institute for Laboratory Astrophysics
University of Colorado and National Bureau of Standards

I. INTRODUCTION

One of nature's curiosities is that cool stars have hot outer atmospheres. In fact, some cool stars have hotter plasma in their coronal exteriors than in their fusion-powered interiors.

The study of exotic atmospheric phenomena in stars was limited until recently to our own Sun. The Sun is a fairly mundane sort of star, as stars go, although the solar surface confronts us with a myriad of constantly changing fine structure that tax the theorist's ingenuity to explain.

The Sun has taught us that the chromosphere and corona are powered by the deposition of mechanical energy. The remarkable temperature inversions in the solar outer atmosphere arising from the dissipation of comparatively small amounts of heat are likely the result of thermal instabilities driven by the inefficiency of the plasma radiative cooling at low densities. The nature of the heating mechanism remains elusive, however, although magnetic fields are thought to play a central role.

Somewhat more than two years ago, the study of cool-star chromospheres and coronae gained a measure of respectability with the advent of the International Ultraviolet Explorer. For the first time, large numbers of cool stars could be observed in the ultraviolet with enough sensitivity to detect the faint emission features formed in the chromosphere ($T \cong 6 \times 10^3$ K) and hotter layers ($T \lesssim 2 \times 10^5$ K) of the outer atmosphere. A year and a half ago, the Einstein soft X-ray telescope was orbited, and almost immediately began detecting coronal emission from ordinary late-type stars. Together, these complementary instruments have provided a remarkable picture of the occurrence of chromospheres and coronae in the HR diagram that is very different from that anticipated by stellar theorists (Vaiana 1980; Linsky 1980).

A few months ago, the Solar Maximum Mission was launched to study solar chromospheric activity at the height of the sunspot cycle.

The detailed morphological and dynamical study of solar active regions by SMM very likely will be a key to understanding many aspects of stellar activity that are seen so vividly with IUE and Einstein. Nevertheless,

†This work is supported in part by NASA under grants NAS5-23274 and NGL-06-003-057 to the University of Colorado.

there is much we cannot learn if we study the Sun in isolation. In particular, the Sun confronts us with an unchanging set of fundamental stellar parameters; surface gravity, effective temperature, chemical composition, age, rotation rate, and so forth. Variations in the gross structure of chromospheres and coronae in stars with very different fundamental properties can, in principle, provide important clues to the nature of outer atmospheric phenomena that studies of the Sun cannot. For example, we might suspect that stellar magnetic fields are the driving force behind the physical structuring and plasma heating in stellar coronae, if the Skylab S-054 soft X-ray images of the solar corona are a useful guide (Vaiana and Rosner 1978), but the origin of the Sun's magnetic field is only poorly understood, and will likely not be explained in the basis of solar observations alone, no matter how detailed.

We must therefore temper the morphological and dynamical picture that solar physicists will provide of our nearby G2 V star with gross surveys of chromosphere-corona properties in a wide range of cool stars, in addition to more comprehensive studies of particularly interesting objects. (I am told that Otto Struve once commented that at least one in five stars is remarkable [e.g. Stencel et al., these proceedings], so there should be no lack of suitable candidates for the latter studies!)

It is in the spirit of the solar-stellar connection, and the supplementing of gross survey results with detailed studies of individual stars, that I present my review.

Because of space limitations I cannot begin to cover all of the IUE studies of cool stars that have been undertaken by the many groups and individuals who are active in this field. (To those authors whose work I do not mention, my apologies.)

Instead, I will focus on three separate topics that together demonstrate the power of IUE for probing the occurrence of chromospheres and coronae in the cool half of the HR diagram, and perhaps also shed some light on the reasons why stellar outer atmospheres behave in the peculiar ways they do.

I summarize the three topics as follows:

First, I will describe how the IUE is used in practice to deduce the physical properties of stellar outer atmospheres. I will discuss the sorts of information that one can extract from low-dispersion and echelle-mode spectra with the SWP and LWR cameras. I will illustrate the discussion with spectra of two bright binary systems, α Centauri (G2 V + K1 V) and Capella (G6 III + F9 III). In fact, the comparison of these two systems with the Sun has revealed unexpected clues to the nature of the chromosphere-corona phenomena. (Harking back to Otto Struve's comment, there should be at least one remarkable star in that group of five, and there is!)

Second, I will describe the several IUE surveys of stellar Mg II emission that are now available. The Mg II h and k resonance lines are important radiative cooling agents in stellar chromospheres, and have provided the first empirical confrontation with a proposed chromospheric heating

mechanism, namely acoustic waves. In addition, the correlations of Mg II emission core shape parameters with stellar luminosity -- the Wilson-Bappu relation for the FWHM for example -- provide useful clues to systematic trends of chromospheric structure with changing stellar properties, especially surface gravity. I will discuss what the stars that obey the Wilson-Bappu effect seem to be telling us about chromospheric conditions, and equally important, how the stars that don't obey the Wilson-Bappu relation fit into the overall picture.

Last, I will summarize some of the recent low-dispersion surveys of cool-star emission in the 1150 Å-2000 Å short wavelength region. Several of the strong emission features found in that region -- C II 1335 Å and C IV 1550 Å for example -- are formed in the thin, 10^5 K transition region (TR) interface between the multi-million degree corona and the 6000 K chromosphere. I will describe the evidence that the cool half of the HR diagram is divided into zones where the TR emission is prominent, and zones where the hot lines tend to be very weak or below detection thresholds. I will present preliminary correlation diagrams comparing the chromospheric emission in the Mg II doublet with the hotter lines of the SWP region, and demonstrate that stars with weak transition regions have weak chromospheres as well. Finally I will speculate on the nature of the chromospheric heating mechanism that is suggested by the Mg II correlations,and review an evolutionary scenario to explain the weakening of cool-star outer atmospheres in the red giant branch.

II. ULTRAVIOLET SPECTROSCOPY WITH IUE

IUE offers the stellar spectroscopist two complementary observing modes: (1) low dispersion, for which no information concerning detailed line profiles or velocities is available, but the resolution is adequate to separate important emission features from each other and from background continua; and (2) the echelle mode, which can provide detailed line profiles with a resolution of somewhat better than 30 km s^{-1}, and individual line positions to within several km s^{-1}. The echelle mode does sacrifice sensitivity for increased resolving power, consequently only a few bright cool stars are accessible, even with long exposures (at short wavelengths). Nevertheless, comparatively faint stars are observed routinely in the Lα region with the low dispersion mode (and at the 2800 Å Mg II resonance lines with the LWR echelle mode).

A. LOW DISPERSION MODE, SHORT WAVELENGTH REGION

Figure 1 compares IUE short wavelength spectra of the nearby solar-type dwarfs of α Centauri (G2 V + K1 V) with an irradiance spectrum of the Sun that has been degraded to the 6 Å FWHM resolution of the low dispersion mode. The solar data were obtained during a moderately active portion of the sunspot cycle (Mount, Rottman and Timothy 1980).

The spectra illustrated in Figure 1, and in several of the subsequent figures, are normalized fluxes. That is, the absolute monochromatic fluxes measured at the Earth have been divided by the stellar bolometric luminosity,

also as measured at the Earth. (The resulting monochromatic units are $Å^{-1}$.) Normalized fluxes are a fair way to compare the chromospheric emission of stars having very different surface areas (dwarfs and giants, for example), and essentially represent the fraction of the stellar irradiance budget that is provided by the particular emission spectra. Normalized fluxes are independent of often uncertain stellar distances, although they are sensitive to bolometric corrections, which can be quite large for K and M stars.

One sees in Figure 1 that the two α Centauri dwarfs are very similar to each other and to the Sun in their ultraviolet emission properties. Both α Cen A and B exhibit all of the important transition region and chromospheric lines seen in the solar short wavelength spectrum (O I 1305 Å, C II 1334 Å, Si IV 1400 Å, C IV 1550 Å, Si II 1815 Å). In fact, the normalized line strengths of α Cen A and B are quantitatively similar to the solar values (Ayres and Linsky 1980a).

The presence of TR emission in both α Centauri dwarfs is proxy evidence that these solar-type stars possess multi-million degree coronae analogous to that of the Sun. In fact, both components of α Centauri have been resolved recently as coronal soft X-ray sources by the High Resolution Imager on Einstein (Golub et al. 1980).

Figure 2 depicts the ultraviolet emission spectrum of another binary system, Capella (α Aurigae A; G6 III + F9 III). Capella has a much shorter orbital period than α Centauri (0.3^y versus 80^y), and the two giants are too close to each other to be separately observed by IUE or Einstein. Consequently, only the composite emission spectrum is obtainable.

While Capella exhibits essentially the same emission features that are prominent in the solar spectrum, the normalized line strengths, particularly of the 10^5 K transition region features, are considerably larger, and several of the line ratios, O I 1305 Å/C II 1335 Å and C I 1660 Å/C IV 1550 Å for example, are quite different. Like the α Centauri system, Capella has been detected as a prominent coronal soft X-ray source by HEAO-1 and Einstein (Cash et al. 1978, Holt et al. 1979).

Given SWP spectra such as those illustrated in Figures 1 and 2, one can determine straightforwardly integrated line strengths, line ratios, and continuum intensity distributions.

Emission line strengths indicate the amount of material present over the temperature range where the particular atom or ion is most abundant. In addition, many of the prominent high temperature emission features accessible to IUE in the Lα region, namely the Si IV, C IV and N V doublets, are important radiative coolants between about 6×10^4 and 2×10^5 K. Consequently, the strengths of these features are an indirect probe of the plasma energy budget in the transition region.

Like the emission line strengths, line ratios play an important role in diagnosing the physical conditions in stellar outer atmospheres. The most common application of line ratios is to estimate transition region densities (Doschek et al. 1978b). In principle, intensity ratios of spectral features

that are formed under similar plasma thermal conditions, but which have different sensitivity to local density — "permitted" and "forbidden" transitions, for example — can be used to deduce the spatially averaged pressures in the atmospheric structures responsible for the ultraviolet emission. However, many obstacles remain in the practical application of density sensitive line ratios (Raymond and Dupree 1978; Baliunas and Butler 1980), particularly because most of the numerical simulations of the response of line ratios to density have been specialized to solar transition region structures (Doschek et al. 1978a). Nevertheless, the density diagnostic line ratio techniques offer essentially the only way to estimate transition region pressures in other stars that is comparatively free of geometrical considerations (the situation of a patchy TR brightness distribution, for example).

The question of transition region pressures is an important one, because it bears directly on the nature of the heating mechanism. The classical (preSkylab) picture of the solar transition region was of a geometrically thin interface between the hot corona and cool chromosphere that supported a large conductive heat flux driven by the steep temperature gradient (Withbroe 1977). The heat conducted from the corona downward into the cooler and denser chromospheric layers was an important energy loss channel that, in concert with high temperature radiative emission, served to stabilize the coronal plasma thermally. When the conductive flux through the transition region is dissipated entirely by radiative cooling, the gas pressure in the TR is proportional to the conductive flux itself (for a plane parallel nondivergent geometry, see e.g., Rosner, Tucker and Vaiana 1978).

Since the conductive flux is proportional to the temperature gradient, and since the emission strength of an optically thin resonance line of an abundant ion in the TR is roughly proportional to the square of the gas pressure divided by the local temperature gradient, then the TR emission should be directly proportional to the gas pressure (e.g., Haisch and Linsky 1976). Consequently, if stellar TRs obey the conductive heating hypothesis, then the stellar TR pressures should scale directly from solar values as the ratio of the stellar and solar surface fluxes of permitted TR lines (Haisch and Linsky 1976). Alternatively, if stellar transition regions are heated by a nonconductive process — magnetic reconnection in situ, for example — then the same surface flux could be provided at considerably lower pressures simply by a flatter temperature gradient In fact, empirical studies of the temperature gradient at the 10^5 K level of the solar TR, by means of emission measure analyses, have revealed that the likely conductive flux in those and deeper layers is insufficient to balance the measured radiative losses, consequently an additional heating agent seems to be required (Withbroe 1977). Furthermore, Noyes (1974) has proposed a semiempirical TR model to explain the intense emission in 10^5 K lines observed in sunspot plumes (Foukal et al. 1974), that is characterized by a much flatter temperature gradient than is predicted by the conductive heating model. It is therefore premature to suppose that all stellar transition regions are a product of conductive heating (e.g., Baliunas et al. 1979), until reliable, independent pressure estimates are available to test that contention in a wide variety of late-type stars.

A third useful aspects of the IUE low dispersion spectra of cool stars is the continuum emission distribution longward of 1500 Å. Radiation in

that spectral region is produced in the stellar outer photosphere, and is a sensitive diagnostic for the stellar effective temperature. For example, the substantial drop in normalized continuum emission levels near 1800 Å between α Cen A and α Cen B is the result of only a 500 K difference in effective temperature. On the other hand, the close similarity in the normalized continuum emission strengths of α Cen A and the Sun indicates that the two G dwarfs have very nearly the same effective temperature. [In several respects, α Cen A and the Sun are twins of each other (Flannery and Ayres 1978).] Finally, the continuum emission levels in the composite low dispersion spectrum of Capella are significantly larger than solar. The ultraviolet continuum enhancement implies that the hotter secondary, which dominates the short wavelength emission of the system, is very likely a late F giant.

In addition to its usefulness as a temperature diagnostic, the short wavelength continuum emission can signal the presence of previously unrecognized stellar companions. For example, Mariska, Doschek and Feldman (1980) have discovered a hot-star companion to the classical cepheid η Aquilae on the basis of an anomalously bright emission signature in the region shortward of 1600 Å that did not vary with the cepheid pulsation period.

B. ECHELLE MODE, LONG WAVELENGTH REGION

Useful as the low dispersion mode is, the stellar spectroscopist should feel somewhat uncomfortable that it does not provide many of the basic pieces of information that are central to atmospheric structure analyses. Principal among these are line shapes and velocities. Fortunately, the IUE echelle modes can provide such information for a wide range of cool stars longward of 2500 Å, and for the few brightest shortward of 2000 Å.

i) Line Shapes

Emission line profiles contain an enormous amount of information concerning plasma conditions in — and the geometry of — the line-forming region.

When a feature is optically thin, one can estimate the amplitude of nonthermal broadening velocities in the layers where the emission originates. For example, Athay and White (1978,1979) and Bruner (1978) have applied this technique to high-quality solar C IV profiles, obtained with the OSO-8 UV spectrometer, to set limits on the possible acoustic wave flux passing through the 10^5 K layers

When a line is optically thick and develops a centrally reversed emission core, one can estimate the optical path length required to produce the central reversal. The line optical depth and total emission can then be used to estimate the plasma density and geometry of the emitting structures. Lites, Hansen and Shine (1980) have applied such an approach to self-reversed C IV profiles observed in an active region near the solar limb by OSO-8.

Some emission features, the 2803 Å h and 2796 Å k resonance lines of Mg II for example, are very optically thick in stellar chromospheres. In

fact, the Mg II features are effectively thick (see Hummer and Stewart 1966) as well. Very optically thick lines that are effectively thick in the chromosphere, and which possess extensive Lorentzian damping wings (H I 1216 Å Lα and the H and K resonance lines of Ca II are other examples) are valuable thermal structure diagnostics (Ayres 1975; Basri et al. 1979). The outer edges of the emission features, beyond the narrow Doppler-dominated core, and the damping wings of these lines carry, in principle, a faithful mapping of the outer atmospheric thermal structure from the middle chromosphere down to the deep photosphere (in the case of Mg II and Ca II). For example, the k_1 profile minimum features are formed near the temperature minimum region at the photosphere-chromosphere interface, while the k_2 emission peaks are formed in the hotter layers of the middle chromosphere, where the Mg II cores first become effectively thick.

The left-hand panel of Figure 3 compares echelle-mode profiles of Mg II k from α Cen A and B. The ordinate is normalized flux, $f_\lambda/\ell bol$, in the same units as Figures 1 and 2.

First, note that the Mg II emission cores are overwhelmingly brighter than any of the chromospheric or transition region features of the short wavelength spectrum (even Lα). Since the Mg II features are important radiative coolants in the stellar chromosphere, one sees that the chromospheric energy budget must be considerably larger than that of the overlying transition region.

Second, note that the inner damping wings of the α Cen A k profile are brighter than the α Cen B k wings. This difference is a reflection of the 500 K photospheric temperature difference of the two dwarf stars, and is analogous to the behavior of the UV continuum emission seen in Figure 1. However, the contrast is amplified near 1800 Å compared with 2800 Å owing to the exponential character of the ultraviolet Planck function.

Despite the cooler photospheric emission, the α Cen B k core is brighter than that of α Cen A (in normalized flux). Consequently the α Cen B chromosphere likely occupies a larger fraction of the overall stellar energy budget than that of α Cen A. A similar difference is seen in the Lα region (Fig. 1), where the α Cen B TR emission features are somewhat brighter than those of α Cen A.

Finally, note that the k-line emission core of α Cen B is narrower at the top, and has a smaller FWHM, than that of α Cen A, although the emission features are more nearly the same width at their bases. The broadening of the k-line FWHM with increasing absolute visual luminosity (α Cen A is $1^m.3$ brighter than α Cen B in M_V) is a well-known correlation that was first recognized in the near ultraviolet Ca II H and K resonance lines by Wilson and Bappu (1957). The existence of such a simple correlation has provided chromospheric theorists with a tantalizing challenge, whose resolution remains controversial even after two decades of study. I will return to the Wilson-Bappu effect, and its bearing on chromospheric structure, later in the review.

ii) Profile Asymmetries and Velocities

Besides the fundamental emission core shape parameters, high resolution observations of the h and k features offer further possibilities for deducing chromospheric structure. For example, under certain circumstances, asymmetries in the emission cores can indicate gross material inflows or outflows (Stencel and Mullan 1980). Furthermore, absorption features superimposed on the intrinsic stellar emission profile can be used to probe the properties of circumstellar (Hartmann, Dupree and Raymond 1979; Stencel et al. 1980) and interstellar matter (Böhm-Vitense 1980a) along the line of sight. Finally, emission centroid velocities and gross asymmetries in the profiles can be used to isolate the component emission in certain moderate and short-period binary systems. Although the separation of the companion stars on the sky may be too small to allow the component spectra to be observed individually, often the projected orbital velocity amplitudes are sufficiently large to permit at least partial resolution of the component spectra by the Doppler effect. This technique is particularly useful in practice, because the closer the two companions are to one another, the faster the orbital motions, and the easier it is to separate the individual spectra (if the orbit is favorably inclined in the line of sight). Furthermore, there is a well-known correlation between orbital period and chromospheric activity levels in cool-type spectroscopic binaries, in the sense that the shortest period systems ($P < 10^d$ RS CVns, for example) tend to exhibit the brightest optical emission lines (Ca II and Hα; see e.g., Young and Koniges 1977), and the strongest coronal soft X-ray emission (Walter, Charles and Bowyer 1978). Nature has indeed been kind to provide a class of interesting close-binary systems that are possible to study with a small aperture instrument such as IUE.

The right-hand panels of Figure 3 illustrate some of these notions more quantitatively.

I have depicted profiles of the Capella Mg II k emission at two orbital phases when the primary and secondary have the maximum, and opposite, radial velocity separations. In both panels the radial velocity scale is relative to the system center-of-mass velocity, and the positions of the primary's and secondary's velocity zeros at each orbital phase are indicated by arrows. The substantial asymmetry in the K-line emission produced by the F-giant secondary is readily apparent. Note also that the Mg II emission envelope of the giant stars is considerably broader than that of the α Centauri dwarfs, as required by the Wilson-Bappu relation.

What appears to be k_3 central reversal in the G-star component of the composite emission profile (bottom, right-hand frame of Fig. 3) is very likely mostly interstellar Mg II absorption. In particular, the deep self reversal in the primary k emission core (Aa) is absent in the upper frame when the primary is to the red of the system center of mass, but an absorption feature is present at the same velocity (-10 km s^{-1} relative to the Capella COM) as the "k_3" feature in the bottom frame. The presence of a strong interstellar Mg II absorption feature is not unexpected, since a prominent interstellar D I Lα absorption is seen against the intrinsic stellar Lα emission (Dupree, Baliunas and Shipman 1977; Ayres and Linsky 1980b).

Nevertheless, the presence of such a strong absorption feature in the center of the k line of a nearby star ($d \cong 13$ pc) is somewhat disconcerting. In particular, the k_2 emission peak separation plays an important role in some theoretical interpretation of the Wilson-Bappu effect, and the red-violet k_2 emission asymmetry has been invoked as a spectral anemometer to measure stellar wind flows (e.g. Stencel and Mullan 1980). However, as Böhm-Vitense (1980a) has shown recently in a systematic survey of interstellar Mg II absorption, in stars more distant from the Sun than a few tens of parsecs, much of the k_3 self reversal and the k_2 peak asymmetry may be an artifact of the interstellar absorption component. In fact, the presence of a saturated interstellar absorption core displaced somewhat from the stellar radial velocity may explain why some supergiants, 56 Peg (KO Ibp) for example, exhibit opposite k_2 peak asymmetries in Mg II and Ca II (Stencel et al. 1980), despite the fact that the two sets of resonance lines are formed at essentially the same levels of the stellar chromosphere, and presumably under nearly similar conditions of temperature, density and macroscopic flow velocity (cf. Basri 1979). (Note, however, that purely circumstellar absorption can produce the same result [see Stencel et al., these proceedings].)

C. ECHELLE-MODE, SHORT WAVELENGTH REGION: THE CAPELLA DICHOTOMY

One has seen from the comparison of low-dispersion, short wavelength spectra that the Capella system is considerably more active than the solar-type stars of α Centauri or the Sun itself. One anticipates that echelle-mode studies of Capella in the short wavelength region might reveal clues to the particular properties of the chromospherically active giant system that sets it apart from the quiescent main sequence stars.

Figure 4 compares the stronger member of the C IV doublet, 1548 Å, and the weakest component of the Si II triplet, 1808 Å, in α Centauri A and Capella. The Capella profiles were taken at one of the orbital velocity crossings when the contributions from the G primary and F secondary are superimposed in velocity.

Note that the α Centauri A profiles are narrower than their Capella counterparts, in fact close to the echelle-mode resolution of $\cong 25$ km s^{-1}. The α Centauri profiles are also considerably fainter than the Capella emission features, as anticipated from the low dispersion spectra.

The enhanced width of C IV 1548 Å, in particular, is likely an artifact of an optically thick emitting region, in contrast to the solar TR which usually is regarded as optically thin in C IV (but see Lites et al. 1980). If the principal broadening mechanism is Doppler in character, either thermal or small-scale velocity fields, an optically thick emitting region can produce a profile that is a factor of $\alpha \cong (\ell n\ \tau_{\ell c})^{1/2}$ wider than the intrinsic Doppler width, where $\tau_{\ell c} >> 1$ is the line center optical thickness of the layer. The scale factor α is a very slowly varying function of $\tau_{\ell c}$, and could provide at least factor of 2 width enhancements for the strongest TR lines of Capella. However, the saturation phenomenon (also called "opacity broadening") is not a convincing explanation for the enhanced Si II 1808 Å width of Capella, since the Si II feature is already optically thick in the solar chromosphere (Tripp, Athay and Peterson 1978), and presumably also in

α Cen A. On the other hand, the Si II feature is likely not thick enough that the Lorentzian wings of the profile function can significantly influence the emission line shape (the wing effect is likely important for the Mg II h and k cores, however). Consequently, the enhanced Si II width in Capella must be explained either by an increase in the intrinsic chromospheric Doppler width, or by an extrinsic Doppler broadening mechanism such as macroscopic flow patterns or rotation.

In short, the significant differences between the gross emission line strengths of Capella and α Centauri A are continued in the details of the individual line shapes. The comparison of line shapes has not directly helped us understand the fundamental differences between the giant stars and the solar-type dwarfs. Nevertheless, the comparison has provided us with at least one potentially useful clue: the transition region of Capella is very likely optically much thicker than the solar TR. (This suggests in fact that the Capella TR is not heat-conduction dominated, since the optical thickness $\tau \sim P/[dT/dh]$ of the conductive equilibrium TR is independent of the TR pressure P, since $[dT/dh] \sim F_{cond} \sim P$, and τ therefore should be the same in Capella as in the Sun.)

An even more important — and unexpected — clue to the nature of the giant-dwarf emission dichotomy was revealed by short wavelength echelle-mode observations of Capella at different orbital phases.

Figure 5 compares several prominent emission features of the Capella short wavelength spectrum at two orbital phases. The profiles in the left-hand panel were taken at one of the orbital velocity crossings when the two stars have the same projected radial velocity, and their spectra are superimposed. The profiles in the right-hand panel were taken near one of the elongations when the F-type secondary is shifted to the red of the system center-of-mass velocity, and the G-type primary is shifted to the blue. The velocity separation is of order 50 km s^{-1}. The zero-points of the individual stellar velocity scales at the two orbital phases are indicated by arrows.

The emission profiles are arranged from bottom to top in a sequence of increasing temperature of formation. The bottom-most and top-most profiles are composites of two or more features that are formed at similar temperatures and have similar line shapes (Si IV 1394,1403 Å + C IV 1548,51 Å, for example). The features were superimposed on a common velocity scale to enhance the signal-to-noise of systematic velocity patterns.

The profiles in the left-hand panel are all comparatively symmetric and the composite Si IV + C IV line shape has essentially the same velocity centroid as the chromospheric O I and Si II features. (The dotted curves are the long wavelength edges of the emission profiles reflected about the system COM velocity to illustrate the symmetry of the line shapes. The error bars within each profile are estimated emission bisectors.) The lack of significant differential shifts between the TR features and the chromospheric lines at the velocity crossing suggests that there are no substantial systematic flows of material at the 10^5 K level in Capella — a wind for example — compared with the cooler chromospheric layers (Ayres and Linsky 1980b). This result is contrary to interpretations of low S/N Copernicus spectra of

Capella (Dupree 1975, 1976), which indicated the presence of a $\cong 30$ km s^{-1} accelerating outflow at and above the 10^5 K level.

The right-hand panel illustrates the most surprising result of the Capella study (Ayres and Linsky 1980b): while the chromospheric features (O, I, Si II) taken near one of the elongations in the orbit are asymmetric, indicating contributions from both the G primary and F secondary, the high temperature composite profile remains comparatively symmetric, and shifts bodily to the red following the radial velocity motion of the secondary, exclusively. The straightforward interpretation of this curious behavior is that most of the high temperature emission from the Capella system is produced by the F-type secondary, rather than by the somewhat more massive and luminous primary. This result is contrary to the presumption of most previous work on the Capella system that the G-star is the major ultraviolet emitter (e.g. Dupree 1975; Haisch and Linsky 1976). In fact, symmetrizing the long wavelength emission edges of the elongation profiles about the secondary's velocity indicates that the bulk of the low temperature, chromospheric emission is produced by the F-star as well.

In short, the Capella-α Centauri emission dichotomy has resolved itself into an emission dichotomy between the Capella giants themselves. This is a promising simplification because the evolved giants are obviously very different from the main sequence dwarfs, but the Capella stars are very similar to one another in their fundamental stellar properties: mass, temperature, luminosity, chemical composition, age, and so forth.

The only fundamental property that is very different between the Capella siblings, and is a plausible candidate to explain the emission dichotomy, is rotation (Ayres and Linsky 1980b). The Capella primary is a sharp-lined, slow-rotating giant, while the secondary has a diffuse spectrum and presumably is a fast rotator. The rotation dichotomy itself is likely a result of the somewhat more advanced evolutionary state of the primary compared with that of the secondary owing to the small mass difference (Iben 1965).

D. THE ROTATION-ACTIVITY CONNECTION

Rotation is a plausible candidate to explain the Capella ultraviolet emission dichotomy, if the chromospheric activity of cool stars is intimately related to surface concentrations of magnetic fields, as certainly appears to be the case for the Sun (Vaiana and Rosner 1978). If the decay of surface fields is responsible for the heating of the outer atmosphere, the fields must be replenished continually for the chromosphere and corona to persist over evolutionary timescales. A likely replenishment mechanism is dynamo action (Parker 1955, 1970), and the dynamo is more vigorous in fast rotating convective stars than in slow rotators. Indeed, the chromospherically most active of cool stars are those in short-period binary systems (the RS CVns, for example; Hall 1978), where tidal friction forces the two companions into rapid, synchronous rotation (Zahn 1977). Furthermore, Bopp and Fekel (1977) have argued that rotation, rather than binarity per se, is responsible for the BY Draconis flare star "syndrome" among dwarf M stars. Finally, the recent Einstein survey of coronal soft X-ray emission (Vaiana 1980; Vaiana et al. 1980) has revealed that the brightest cool-star sources, as a class, are the

F-type stars. These tend to be fast rotators compared with single G, K and M stars, very likely because the F stars are young (see e.g. Skumanich 1972).

Ironically, the corona itself is thought to be responsible for the spin-down of single stars as they age. In particular, a weak coronal breeze, such as the solar wind, that is magnetically coupled to the stellar photosphere out to many radii, can shed angular momentum effectively (Durney 1972). If the magnetic braking by a coronal breeze is positively correlated to the chromospheric activity level, then the corona is, in a sense, a self-defeating entity. However, short-period binary systems need not suffer the coronal decay of single stars, owing to the large reservoir of angular momentum in their orbits to maintain the component rotation rates through tidal coupling.

Finally, the rotation-activity connection has an intriguing, practical consequence. Soft X-ray and EUV images of the Sun have revealed that active regions are composed of discrete structures, namely magnetic loops (Rosner, Tucker and Vaiana 1978). If the analogous loop systems on an active star extend an appreciable fraction of the stellar radius above the photosphere, and if the loops corotate with the phtospheric plasma, one might expect enhanced broadening of TR (and coronal) emission features, compared with chromospheric or photospheric line profiles. Furthermore, if a particularly active -- or flaring -- loop system happens to be near one of the equatorial limbs, one might find an emission enhancement in the wing of the C IV 1548 Å profile, for example, that corresponds to the projected rotational velocity of the active region at the time of observation. Again nature has provided a simple way to obtain crude spatial information concerning structures on the surface of another star. All one requires is moderate spectral resolution, which is certainly more appealing from a practical standpoint than the alternative: direct imaging with kilometer-aperture telescopes!

III. MG II h AND k: CHROMOSPHERIC COOLING AND WIDTH-LUMINOSITY CORRELATIONS

Turning aside from stellar transition regions for the moment, I would like to discuss Mg II emission in more detail, particularly with regard to chromospheric radiative losses, and the origin of the Wilson-Bappu relations.

A. CHROMOSPHERIC COOLING BY MG II h AND k

Mg II h and k are important radiative cooling agents in stellar chromospheres (Linsky and Ayres 1978). Calibrated measurements of the integrated core emission of these lines provide a more-or-less direct probe of chromospheric energy budgets. In fact, comparisons of pre-IUE Mg II fluxes with the predictions of chromospheric heating by acoustic waves constituted the first direct test of a proposed theoretical chromosphere formation mechanism (Linsky and Ayres 1978).

The important result from the early Mg II work was that when expressed in the form $f_{Mg\ II}/\ell_{bol}$, the stellar emission fluxes showed a wide range of variation at a given spectral type and luminosity class, but no clear correlation with surface gravity. The empirical result was diametrically opposite to the predictions of the acoustic heating scenario. The latter required

rather uniform chromospheric heating (and consequently also uniform Mg II cooling) at a given spectral type and luminosity class, because only convection zone parameters -- T_{eff} and g -- ultimately determined the acoustic flux production. Furthermore, the acoustic theory predicted a large systematic increase in the heating with decreasing surface gravity (e.g. Ulmschneider et al. 1977). Some attempts have been made recently to rectify the substantial discordances between the acoustic heating theory and the semiempirical chromospheric cooling estimates (Schmitz and Ulmschneider 1979; Böhm 1980), but the fundamental disagreement remains (Linsky 1980). The failure of the acoustic heating scenario to explain the formation of stellar chromospheres is no surprise to solar physicists, given the overwhelming empirical evidence that the structure of the solar outer atmosphere is intimately related to magnetic fields (Skumanich, Smythe and Frazier 1975; Vaiana and Rosner 1978), which are not even considered in the conventional acoustic heating treatments.

In any event, IUE has provided a greatly expanded data set to test proposed chromospheric heating mechanisms. For example, Basri and Linsky (1979) and Stencel et al. (1980) have presented diagrams analogous to that of Linsky and Ayres, but based on the more homogeneous and better calibrated IUE spectra. Furthermore, Böhm-Vitense and Dettmann (1980) recently have published an extensive survey of F and late-A stars to probe the occurrence of classical chromospheres in the HR diagram. Mg II fluxes for additional stars are available elsewhere (e.g. Hartmann, Dupree and Raymond 1980; Pagel and Wilkins 1979).

I have combined these several IUE studies of Mg II emission on a common diagram in Figure 6. The "bubbles" represent mean $f_{MG\ II}/\ell_{bol}$ ratios in each of the spectral type/luminosity class bins for which data are available. Often, only one star falls in a bin, but in some cases, particularly in the K-giant region, as many as ten stars are represented by a single bubble. The small filled circles refer to stars for which Mg II emission was not detected (these data are taken from the Böhm-Vitense and Dettmann study). The dashed circles are Mg II flux ratios based on the Copernicus work of Weiler and Oegerle (1979) as quoted by Basri and Linsky. The Copernicus fluxes are very uncertain compared with the IUE measurements. I have included them only to fill out regions of the bubble diagram where IUE measurements were not available.

The Mg II bubblegram illustrates three important characteristics of the occurrence of chromospheres in the HR diagram.

First, there is an abrupt onset of detectable chromospheric emission in the early F stars that coincides with the beginnings of vigorous convective activity (see Böhm-Vitense and Dettmann for details).

Second, there is no large systematic trend of increasing $f_{Mg\ II}/\ell_{bol}$ ratios with increasing luminosity, although the variation of flux ratios within a given bin (not illustrated in Fig. 6 explicitly) can be an order of magnitude or more. For example, the active G8 dwarf ξ Boo A has a Mg II flux ratio (Basri and Linsky 1979) some twenty times that estimated from the Pagel and Wilkins (1979) h and k profiles of the G8 dwarf τ Ceti. Therefore, the

new IUE Mg II spectra confirm the tentative results of the earlier Linsky and Ayres study.

Third, the stars in the red giant branch (KO III and later) appear to exhibit somewhat weaker chromospheric Mg II emission ratios than the dwarfs or supergiants of similar spectral type (see also Stencel et al. 1980). This is in fact the same region of the HR diagram where Linsky and Haisch (1978) identified an abrupt drop in transition region emission, which they interpreted as a weakening, or disappearance altogether, of solar-like coronae. Incidentally, the Linsky-Haisch division corresponds to the onset of strong stellar winds in the red giants ($\dot{M} \cong 10^{-8}$ $M_\odot$ yr^{-1} compared with $\dot{M} \cong 10^{-14}$ for the solar "breeze"), and has been characterized as a corona-wind boundary (Haisch, Linsky and Basri 1980).

I will return to the question of the origins of the structure seen in the Mg II bubblegram at the conclusion of the review.

B. THE WILSON-BAPPU RELATIONS

Because the Ca II H and K and Mg II h and k transitions are so similar in their atomic properties, it is not surprising that the systematic increase of H and K emission core FWHMs with increasing stellar luminosity -- the well-known Wilson-Bappu effect -- is seen in the Mg II features as well (Moos et al. 1974; McClintock et al. 1975; Dupree 1976). The study of the Wilson-Bappu effect is somewhat easier in the Mg II lines than in Ca II since the former always exhibit much larger core-wing contrasts than the latter. Furthermore, a large (and still growing) sample of high-quality Mg II line shapes has been obtained by one instrument, namely IUE. A homogeneous data set is an essential ingredient for determining systematic trends in line profile shapes.

Although the conventional Wilson-Bappu effect refers solely to the broadening of the emission core FWHM (Lutz 1970), other characteristic profile features, such as the K_1 minimum separation and K_2 peak separation (see Fig. 7), also obey qualitatively the same width-luminosity correlations as the FWHM (Ayres, Linsky and Shine 1975; Cram, Krikorian and Jefferies 1979). Curiously, though, the Mg II and Ca II profiles of solar active regions, which exhibit 5-10x enhanced chromospheric emission compared with "quiet" regions, are broader at the base (WK_1), but narrower at the emission peaks (WK_2), while the FWHM is essentially unchanged (Shine and Linsky 1972). In fact, the constancy of the Ca II FWHM among stars of similar absolute visual magnitude, but very different chromospheric activity levels, allows the Wilson-Bappu effect to be a reliable luminosity indicator, on the one hand, but a headache for theoretical modelers, on the other (see e.g. Böhm-Vitense 1980b).

The simple dependence of the K (and k) FWHMs on stellar luminosities, and little else, suggests that the fundamental correlation is in terms of stellar surface gravity (e.g. Lutz and Pagel 1979).

i) Doppler versus Damping Control

There are essentially two kinds arguments to explain why the Ca II and Mg II FWHMs broaden with decreasing surface gravity. The first class of arguments assumes that the emission core shapes are controlled entirely by nonthermal Doppler broadening, and the widening of the emission profiles with decreasing surface gravity simply reflects a systematic increase of chromospheric nonthermal velocities with increasing stellar luminosity. The second class of arguments assumes that the outer edges of the emission core are at least partially controlled by the Lorentzian damping wings, and that the overall broadening of the emission profile is caused by a physical thickening of the stellar chromosphere with decreasing surface gravity. [Previous work on both aspects is summarized by Ayres (1979).]

The Doppler hypothesis would seem to be plausible if, for example, the Mg II emission cores were broadened by acoustic waves having roughly the same flux in dwarf and giant stars. Since the acoustic flux is proportional to the square of the disturbance amplitude v and to the material density ρ, one would expect v to increase with decreasing surface gravity to compensate for the substantial drop in ρ. However, in the supergiant stars, which have very wide Mg II emission profiles, nonthermal velocities greatly in excess of the chromospheric sound speed would be required to explain the observed broadening (Basri 1979). It is not clear how this "shocking" result could be attained in a real stellar chromosphere. Furthermore, it is difficult to reconcile the k_1 width-luminosity relation in the Doppler context, since the profile minimum features are formed well beyond the chromospheric Doppler core (Engvold and Rygh 1978). Finally, the narrowing of the K_2 emission peak separation in solar plages compared with quiet Sun profiles, but relatively unchanged FWHM, are difficult to understand in the pure Doppler picture, unless the nonthermal broadening decreases rapidly with altitude in active regions, contrary to semiempirical chromospheric models (Shine and Linsky 1974).

The second class of Wilson-Bappu explanations, based on the hypothesis of damping wing control in the outer emission core, relies on a physical thickening of stellar chromospheres as surface gravity decreases. In the damping wings, the monochromatic opacity is a slowly varying function of wavelength displacement ($\kappa_{\Delta\lambda} \sim \Delta\lambda^{-2}$), at least compared with that of the Doppler core ($\kappa_{\Delta\lambda} \sim \exp -(\Delta\lambda/\Delta\lambda_D)^2$). As a result, there is a one-to-one correspondence between wavelength displacements in the profile and atmospheric column densities, in the sense that the intensity at a particular $\Delta\lambda$ is a mapping of the emissivity $\eta(T)$ at monochromatic optical depth $\tau_{\Delta\lambda} \cong 1$ (i.e. an Eddington-Barbier relation; see e.g. Ayres 1979). For example, the temperature minimum at the photosphere-chromosphere interface would be mapped onto an intensity minimum (i.e. K_1) at a wavelength displacement from line center $\Delta\lambda_*$ such that the monochromatic optical depth down to the location of the T_{min} in mass column density, m_* (g cm^{-2}), is of order unity. If T_{min} is shifted to larger column densities, then $\Delta\lambda_*$ will increase as well ($\Delta\lambda_* \sim m_*^{1/2}$). The correspondence between structure in the atmospheric emissivity, which is characterized in terms of the line source function S_ℓ, and features in the emergent profile is illustrated in Figure 7.

The notion that stellar chromospheres might physically thicken in column density with decreasing surface gravity is appealing, particularly because stellar photospheres exhibit just that behavior (at least when they are in hydrostatic equilibrium), owing to the pressure sensitivity of the dominant continuous opacity source, H^- (e.g. Ayres et al. 1975). In fact, Lutz, Furenlid and Lutz (1973) have invoked the photospheric thickening mechanism to explain the gross broadening of the photospheric wings of Ca II H and K with increasing stellar luminosity. It remains, then, to find a mechanism to similarly thicken stellar chromospheres.

There are in fact several possibilities (e.g. Thomas 1973), but I will summarize here only the one proposed by Ayres (1979), if only because I have read that paper somewhat more carefully than the others.

ii) Chromospheric Scaling Laws

In that study, I proposed a set of simple scaling laws for the thickness and mean electron density of stellar chromospheres as functions of, primarily, surface gravity g and an activity scale parameter $\tilde{F}$. The latter indicates by how much a given stellar chromosphere deviates from the gravity-independent mean heating trend I adopted from the Linsky-Ayres Mg II study (see §IIIA, above). For example, $\tilde{F} = I$ for the quiet Sun, while $\tilde{F} \cong 5$ for a medium strength plage.

The scaling laws are predicated on the notion that the initial temperature inversion at the base of the chromosphere is caused by an instability in the low temperature plasma cooling when a source of mechanical heating is present. The thermal instability is driven by the dependence of the plasma radiative cooling (ergs cm^{-2} g^{-1}) on the electron density, and the fact that the electron density itself depends strongly on temperature only between about 5×10^3 K and 8×10^3 K, while for lower and higher temperatures n_e is directly proportional to the hydrogen density n_H. For example, at low temperatures ($T < 5 \times 10^3$ K), electrons are provided by the first ionizations of the abundant metals Fe, Si and Mg (Vernazza, Avrett and Loeser 1976), consequently $n_e \cong 10^{-4}\ n_H$, where the proportionality constant is the collective abundance of those metals. Similarly, above 8×10^3 K, hydrogen is essentially fully ionized, consequently $n_e \cong n_H$. In either regime, the electron density, and therefore also the radiative cooling, is inextricably bound to the rapid outward decrease of the hydrogen density in a hydrostatic stellar atmosphere.

If the atmospheric energy balance is dominated by radiative emission and absorption (radiative equilibrium), the rapid outward decline of the plasma cooling when n_e is proportional to n_H is of little consequence because the radiative heating rate also declines in proportion to the electron density. A balance can thereby be struck between the radiative heating and cooling at comparatively low temperatures ($T < 5000$ K). However, if the atmosphere supports a small mechanical heat deposition, in addition to the radiative absorption, that does not fall off with height as n_H or faster, then at some altitude the mechanical deposition will become comparable to the radiative heating. The combined energy input will then exceed the plasma's ability to cool itself at low temperature, in the face of the rapid outward decline of

the electron density. A thermal instability will ensue, and the plasma will heat up until partial ionization of hydrogen liberates enough additional electrons that the radiative cooling function can balance the mechanical heat input. In the regime of partial ionization of hydrogen, the electron density is at least temporarily divorced from the outward decrease of the hydrogen density. For example, the electron density can remain constant with height while n_H decreases by four orders of magnitude, as long as the temperature rises slowly outward. The atmospheric layers in which the electron density is relatively unchanged and the temperature rises smoothly outward over a four order of magnitude decrease in the gas pressure is what I would characterize as the classical chromosphere. However, once the temperature reaches 8000 K what I would characterize as the electron density is again inextricably tied to the outward hydrostatic decrease of the hydrogen density, and a second thermal instability and temperature inversion -- the transition region -- is possible.

In short, I propose that the gross structure of stellar chromospheres is a simple consequence of the trifurcated character of the n_e/n_H ratio for $T < 10^4$ K, and the sensitivity of the plasma cooling to the electron density.

If one assumes that the energy deposition per gram of material in the chromosphere is constant with height, and that the total heat deposition is the same in a dwarf and a giant star of similar activity levels (namely, the same $f_{Mg\ II}/\ell_{bol}$ ratios at a given T_{eff}), then it is easy to show that the chromosphere of the low gravity giant must be thicker in column density than that of the high gravity dwarf. However, the dwarf star chromosphere requires a larger mean electron density than that of the giant star to ensure that the total radiative cooling will be the same. If one considers two stars of similar surface gravity but different activity levels, one finds that the chromosphere must thicken in the active star, and the mean electron density must increase as well.

The simple chromospheric scaling laws I proposed have profound implications for the Wilson-Bappu effect, if the characteristic profile features -- the K_1 minima and K_2 emission peaks -- are at least partially controlled by the Lorentzian damping wings.

For example, the K_1 minimum feature separation broadens with increasing chromospheric thickness, because the monochromatic optical depths down to the temperature minimum increase in proportion to the column density. Furthermore, the K_2 emission peak separation widens with decreasing mean electron density because the line source function thermalizes to the chromospheric Planck function at larger line-center optical depths, and consequently is mapped onto emission maxima further away from line center. (Note, the so-called thermalization depth, or scattering length, Λ depends inversely on the collisional destruction probability ε, which itself is proportional to n_e. In a chromospheric having an outward temperature rise, Λ is the line-center optical depth at which the source function S_ℓ is a maximum [see Fig. 7]. The maximum of the source function is mapped onto the line profile as a pair of emission peaks in a completely analogous way to the mapping of the source function minimum at T_{min} onto the K_1 intensity minima.)

Consequently, both the K_1 and K_2 feature separations should broaden with decreasing surface gravity, in fact with the same $g^{-1/4}$ behavior. One would therefore expect that profile positions between K_1 and K_2, the FWHM in particular, would show a similar $g^{-1/4}$ gravity dependence.

For stars of similar surface gravity but different activity levels, the situation is somewhat changed. The K_1 feature separation widens with increasing activity as the chromosphere becomes thicker. However, the K_2 peak separation becomes narrower with increasing activity because the larger mean electron density in the active chromosphere forces the line source function to thermalize at shallower optical depths, and consequently to be mapped onto K_2 peaks that are closer to line center. In fact, the K_1 broadening and K_2 narrowing have equal, but opposite, dependences on the activity scale factor $\widetilde{F}$. Consequently, one expects the FWHM to be relatively independent of activity. These behaviors are illustrated schematically in Figure 8.

Although my arguments are perhaps overly simplistic, they do make definite predictions that can be tested.

iii) Confrontation with IUE Observations

The major parameter dependence of the derived width-luminosity scaling laws is the broadening of the K_1 feature separation with decreasing surface gravity, namely $\Delta\lambda_{K1} \sim g^{-1/4}$. What is true for Ca II K_1 is equally true for Mg II k_1.

Figure 9 compares measured Mg II k_1 widths (Basri and Linsky 1980; Stencel et al. 1980) with estimated stellar surface gravities. Since the theoretical k_1 widths also depend on the activity parameter $\widetilde{F}$, stellar metallicity and effective temperature, I have applied appropriate corrections determined from the original scaling laws (Ayres 1979) to isolate the gravity dependence (see also Linsky et al. 1979). The activity parameter is straightforward to derive from measured $f_{Mg\ II}/\ell_{bol}$ ratios, and is usually the largest component of the correction. The adjustments for T_{eff} and nonsolar metallicity are less secure, but are small in most cases. More important, any errors introduced by uncertainties in the k_1 adjustments pale beside the uncertainties in the stellar surface gravities themselves.

Two sets of data are represented in Figure 9. The open and filled circles and open squares depict stars for which both high-quality Mg II k and Ca II K line shape parameters are available, and for which reasonable surface gravity estimates could be found (see Basri and Linsky, and Stencel et al. for details). These data will appear in subsequent diagrams that compare the k and K lines against each other. (I have separated the stars crudely into dwarfs [V], giants [IV,III] and supergiants [II,I].) The pluses represent additional gaints and supergiants from the Stencel, et al. lists for which Mg II k line shape parameters and surface gravity estimates are available, but no Ca II information. I have included these stars in the diagram to give a better impression of the true scatter of the data.

The four-pointed open circles refer to quiet and active Sun profiles of k obtained with the French experiment on OSO-8 (courtesy P. Lemaire; see

Chapman 1980). The plage k_1 separation is larger than that of the quiet Sun, but when corrected for an activity enhancement of $\widetilde{F} = 5$, it actually falls somewhat below the quiet Sun width. (Notice that I have plotted the adjusted k_1 widths in km s^{-1} to partially mollify the Doppler broadening enthusiasts.)

Finally, I have drawn a line with slope -1/4 through the quiet Sun point to illustrate the gravity dependence expected from the simple scaling laws.

It is clear from the figure that while the stars appear to obey a gross trend of increasing k_1 width with decreasing surface gravity compatible with the scaling laws, there is a great deal of scatter, and the lowest gravity stars appear to deviate significantly from the expected relation. Analogous studies of the Ca II K_1 width-luminosity correlation have proposed a gravity dependence closer to -1/5 than -1/4 (e.g. Cram et al. 1979), and a somewhat flatter relation would appear to be appropriate for Mg II k_1 here as well. The departure of the supergiants from the proposed relation is not unexpected, because a subtlety in the k-wing formation process -- partial coherent scattering (e.g. Ayres 1975) -- was glossed over in the derivation of the scaling laws. The density-sensitive coherent scattering effects become increasingly important the lower the surface gravity, and work in the direction of producing a narrower k_1 separation than if the wing scattering were completely noncoherent (see Basri 1979).

iv) The Stars that Don't Obey the Wilson-Bappu Effect

In any event, it is not clear whether the Mg II Wilson-Bappu relation is relevant to the supergiants in the first place. For example, α Ori (M2 Iab) and β Dra (G2 II) have similar Mg II FWHMs, yet the former is some 4 magnitudes brighter in M_V. Furthermore, ζ Cyg (G8 IIIp) is somewhat more luminous in absolute visual magnitude than β Dra, yet has a Mg II FWHM only half as large, and in fact comparable to that of α Ser (K2 III) which is 2 1/2 magnitudes fainter than ζ Cyg in M_V.

Incidentally, another class of stars that do not obey the Wilson-Bappu relations are the short-period eclipsing binaries (e.g. Young and Koniges 1977). In such systems, the Ca II and Mg II FWHMs are correlated with the emission core strength, contrary to a central tenet of the Wilson-Bappu effect that the FWHM is independent of chromospheric activity levels. However, the Ca II and Mg II features of such systems are broadened by the rapid synchronous rotation of the binary companions (at least for the eclipsing systems, which are viewed edge on). The violation of the Wilson-Bappu relation in these cases is simply an expression of a stronger driving force, namely the rotation-activity connection. (This is also a situation in which the Doppler advocates are correct, although the broadening is extrinsic rather than intrinsic.)

v) Mg II k_1 Versus Ca II K_1

Figure 10 compares Mg II k_1 separations with the corresponding K_1 widths in the available sample of dwarfs, giants and supergiants. Ca II

data were taken from the recent surveys by Linsky et al. (1979) and Cram et al. (1979).

The scaling laws predict that the k_1/K_1 width ratio should depend only on atomic parameters and the Mg/Ca abundance ratio. For solar abundances (Mg/Ca $\cong$ 15), the W_{k1}/W_{K1} ratio (when the W's are in Å) should be 2.5. On the other hand, if the minimum features are formed in the Doppler core, it is easy to show that the expected width ratio is about 0.75. The empirical relation in Figure 10 lies comfortably between the alternative predictions.

To explain the apparent discrepancy in terms of the scaling laws requires either a Mg/Ca abundance ratio roughly half of the accepted solar value, which seems unlikely, or a mechanism that would selectively narrow the Mg II k_1 separation relative to Ca II K_1. One possibility is the difficulty of defining the location of the relatively flat k_1 minima in typical IUE LWR echelle spectra, particularly because the Mg II wings are significantly more distorted by atomic line blanketing than are the Ca II inner wings. However, the high-resolution OSO-8 Mg II profiles from the quiet and active Sun exhibit the same overall discrepancy, and the solar k_1 and K_1 feature separations are far less ambiguous than typical stellar data. A more plausible differential broadening possibility is the coherent scattering phenomenon mentioned previously. Coherent scattering has a stronger influence on the Mg II wings compared with those of Ca II, owing primarily to the existence of the subordinate infrared triplet in Ca II which introduces an additional source of noncoherence in the photon scattering and redistribution process that is not available to Mg II h and k (e.g. Ayres 1975).

If one were feeling particularly charitable, one would use the solar width ratios to "calibrate" the magnitude of the differential coherent narrowing effect, namely $Wk_1/WK_1 \cong 1.5$-2.0, and conclude that the remaining stellar width ratios were reasonably consistent with the revised prediction. It is encouraging that the largest deviations from the original prediction occur for the supergiants where chromospheric densities are lowest and the coherence effects largest, while the smallest deviations occur for the high gravity dwarfs where the coherence effects should be least.

vi) Mg II k_2 Versus Ca II K_2

Figure 11 compares Mg II emission peak separations with those of Ca II. The prediction of the Damping hypothesis is depicted as a dotted line, while that of the Doppler hypothesis is depicted as a dashed line. (A height-independent chromospheric Doppler width is assumed for both cases: Yes, the K_2 separation in the Damping picture does depend on the non-thermal broadening, through its effect on the line-center optical depth scale, but only as $v^{1/2}$.)

Although the empirical data appear to be in better agreement with the Damping hypothesis, the comparison is somewhat more ambiguous than that for the K_1 features. Unlike the profile minima, the Ca II and Mg II emission peaks are formed at different heights in the chromosphere. In principle, if the broadening velocity is larger in the k_2 forming region than in the K_2 layers, the Doppler prediction would be increased. Furthermore, the presence

of saturated interstellar Mg II absorption components in the emission core potentially could produce a spuriously large empirical k_2 separation.

vii) Summary

I have presented the Mg II width-luminosity correlations to illustrate several points. First, the Damping hypothesis provides a viable alternative to the conventional Doppler arguments, that mimics quite naturally several aspects of the Wilson-Bappu relations which the Doppler theories are hard-pressed to explain. Second, the comparision of empirical line widths to the predictions of chromospheric scaling laws, for example, is hampered not so much by the poor quality of the measured profiles (which previously was the case), but rather by a lack of reliable stellar parameters, particularly surface gravity. Finally, the optically thick emission cores of Ca II K and Mg II k contain a great deal of information concerning the gross structure of stellar chromospheres that is only just beginning to be tapped.

IV. EMPIRICAL CORRELATIONS AMONG CHROMOSPHERIC, TRANSITION REGION AND CORONAL EMISSION

The final topics I will address are empirical correlations among chromospheric, transition region and coronal emission, and the implications of these correlations for understanding the occurence of chromospheres and coronae in the HR diagram.

As mentioned previously, in the first year of IUE Linsky and Haisch (1978) discovered an apparent division in the HR diagram between stars that tend to exhibit solar-like transition region emission (i.e. C IV 1550 Å) and stars for which the 10^5 K lines are very weak or below detection thresholds. However, stars in the latter category often appear to have prominent chromospheric emission spectra (e.g. O I and Si II). The Linsky-Haisch work generated considerable controversy, particularly concerning whether the division, which the authors characterize as a corona-wind boundary (Haisch et al. 1980), is "sharp" or "fuzzy" (e.g. Dupree and Hartmann 1980). Indeed, Hartmann, Dupree and Raymond (1980) found two hydrid cases of G-type supergiants (α and β Aqr) for which a strong chromospheric wind appears to coexist with hotter, TR-like material. These examples suggest (e.g. Linsky 1980) a multi-component situation analogous to that of the solar outer atmosphere where the structures that emit TR and coronal radiation (the closed magnetic loop systems of active regions) are physically distinct from the structures that produce much of the solar wind (coronal holes, which are regions of diverging magnetic fields).

It is worthwile, then, to reexamine the question of TR boundary lines in the HR diagram, and correlations between TR and chromospheric emission in general, in light of the much larger sample of ultraviolet spectra available today.

A. EMPIRICAL EMISSION CORRELATIONS

The observations I will summarize below are described in more detail by Ayres, Marstad and Linsky (1980). Some ultraviolet data have been taken from other surveys, for example that by Böhm-Vitense and Dettmann (1980) for many of the F stars, and Hartmann et al. (1980) for 3 G-K supergiants. The stellar soft X-ray

measurements are partly from the HEAO-1 experiment and partly from preliminary results of Einstein IPC imaging that were kindly made available through a collaborative observing program with the CFA Stellar Survey team (see e.g. Ayres et al. 1980 for details).

Figure 12 compares the normalized emission strengths of prominent chromospheric and transition region emission lines, and broad-band soft X-ray fluxes (0.15-4.5 keV) as functions of normalized Mg II fluxes. The stars are separated crudely according to spectral type (i.e. warm or cool) and luminosity class (i.e. dwarfs or giants). No finer separation is practical at this stage owing to the limited sample. The four-pointed open circles refer to measurements of the quiet and active Sun as described by Ayres et al. (1980).

Beginning with the chromospheric O I triplet (1305 Å) in the upper left-hand panel of Figure 12, one sees that the O I flux ratios are well-correlated with Mg II, and that the slope of the correlation is roughly unity. However, the giant stars tend to have systematically larger O I fluxes at a given Mg II flux level than the dwarf stars. I conclude that O I is a genuinely "chromospheric" diagnostic, but that the mean atmospheric density plays an important role in setting the overall strength of the oxygen emission. Such a link is plausible because the O I triplet lines are thought to be strongly pumped by H I Lβ, through a Bowen fluorescence mechanism, and the pumping should increase substantially with decreasing chromospheric density (Haisch et al. 1977).

The upper middle panel illustrates the comparison between the Si II triplet (~1815 Å) and Mg II. Here again one finds a close correlation between the two chromospheric features, although the overall emission levels in Si II are a factor of ≅30 smaller. The weakness of Si II relative to Mg II is a reflection of the dominant role played by h and k in the chromospheric radiative cooling.

The top right-hand panel compares the C II doublet (1335 Å) with Mg II. Once again the correlation is strong, at least among the cooler dwarfs and giants, although the slope of the correlation appears to be steeper than for the purely chromospheric O I and Si II features. Curiously, the F stars deviate substantially from the mean trend, in the sense that their C II emission is enhanced relative to Mg II. Since C II is formed in the lower portion of the transition region, it is not surprising that the correlation with Mg II does not have unit slope. Presumably one is seeing the differences between an optically thick layer (the upper chromosphere) and an optically thin layer (the TR) that are at essentially the same gas pressure (e.g. Haisch and Linsky 1976). The fact that a correlation exists at all is compelling evidence that the TR and chromosphere are physically linked in some way, presumably by magnetic fields or a common heating mechanism.

The lower left-hand panel compares the He II Balmer α line (1640 Å) and Mg II. Again one finds an excellent correlation, but apparently of even steeper slope than that of C II. Although He II is formed at only somewhat hotter levels of the TR than C II, photoionization of helium by coronal radiation fields is thought to play an important role in the He I-He II ionization balance (Avrett, Vernazza and Linsky 1976). In fact, Hartmann et al. (1980) have proposed that the He II flux is an indirect diagnostic for the level of coronal soft X-ray emission, namely $F_X \cong 50\ f_{He\ II}$. Some support for that suggestion is found in the steep slope of the He II-Mg correlation (but see below).

The middle, bottom panel compares the summed fluxes of Si IV 1400 Å, C IV 1550 Å and N V 1240 Å with Mg II. The three transition region doublets are formed over a temperature range of 0.6-2 x 10^5 K, and the sum is usually dominated by C IV (10^5 K). Here, one finds a very similar behavior to that of C II. The cooler stars exhibit a good correlation of the hot line flux with Mg II, having a steeper than unit slope, while the F stars deviate systematically from the mean trend. Furthermore, even for the most active stars of the sample (the RS CVn systems HR 1099 and UX Ari), the summed TR fluxes are at least an order of magnitude smaller than the corresponding Mg II fluxes. This dichotomy implies that the chromospheric energy budget in "normal" stars is always considerably larger than that of the overlying TR.

The final panel compares coronal soft X-ray emission levels with Mg II. (A larger, and more systematic, study of X-ray-Mg II correlations is currently in progress [Zwaan 1980]). Again a rough correspondence of increasing X-ray flux with increasing Mg II flux is apparent, although the slope is steeper than any of the previous correlations. However, several of the stars for which only upper limits are available (primarily G-K supergiants) seem to fall well below the mean trend, which is based largely on G-K dwarfs and G giants. For example, the upper limit that falls below the lower edge of the diagram refers to the bright K2 giant Arcturus. That nondetection should be compared with the detection of the K1 giant β Gem (the filled circle immediately above the "3") at normalized flux levels an order of magnitude higher despite the somewhat smaller Mg II flux ratio. It is likely not coincidental that the stars which were not detected in the collaborative mini-survey all show evidence for stellar winds and circumstellar envelopes.

Curiously, the soft X-ray flux levels in the brightest coronal sources exceed the corresponding Mg II fluxes. In those stars, the coronal energy budget must be comparable or larger than that of the chromosphere, whereas in the quiescent dwarf stars, such as the Sun, the coronal energy budget is only a small fraction of the chromospheric budget.

Finally, one sees that the He II-soft X-ray scaling proposed by Hartmann et al. (1980) is incompatible with the measured flux levels, except perhaps for the brightest of the coronal sources. For example, Hartmann et al. predicted that α Aqr (G2 II) would have a soft X-ray flux in the 1/4-keV band of order 7 x 10^{-12} ergs cm^{-2} s^{-1} at the Earth based on the measured He II flux of ≅2 x 10^{-13}. However, the 3σ upper limit for the entire 0.15-4.5 keV Einstein IPC band is only 2 x 10^{-13}, which is considerably smaller than the predicted flux. A similar situation exists for β Aqr, where the measured He II flux is comparable to the Einstein upper limit, whereas the soft X-ray flux should be a factor of ≅50 larger according to the Hartmann et al. prescription. There are at least two ways to resolve the dilemma.

First, circumstellar material surrounding both α Aqr and β Aqr may heavily attentuate the intrinsic coronal soft X-rays, consequently the upper limits measured at the Earth may have little meaning. However, note that the Sun exhibits only 4-7 times enhanced soft X-ray emission relative to He II in both quiet and active regions, contrary to the factor of $\cong$50 expected. Even if circumstellar obscuration is viable for the supergiants, one would still have to find an additional mechanism to explain the solar discrepancy.

A second, more plausible, possibility is that the He II emission strength is itself overestimated, especially in the stars having weak coronae. This possibility is attractive because the "He II" feature is actually a blend of He II and Fe II. Consequently, the intrinsically steep He II-Mg II correlation predicted by the Hartmann et al. prescription (namely $f_{\text{He II}} \cong 0.02 f_X \sim f_{\text{Mg II}}^3$) may be significantly diluted by a $f_{\text{Fe II}} \sim f_{\text{Mg II}}^1$ contribution at moderate and low $f_{\text{Mg II}}/\ell_{\text{bol}}$ levels. Note that the Fe II component is at least 30% of the total He II emission in the Sun (Kohl 1977). The composite relation might then mimic the empirical He II-Mg II slope of 2.

In any event the possibility of either mechanism -- circumstellar obscuration or Fe II contamination -- urges caution in the practical application of the Hartmann et al. He II-soft X-ray scaling prescription.

B. IS THE CORONA-WIND BOUNDARY REAL?

The apparent correlations among chromospheric, TR and coronal emission imply that transition regions and coronae do not completely die out to the right of the Linsky-Haisch boundary. Nevertheless, the weakening of transition regions and coronae in the red giant branch is a real phenomenon that is seen clearly even in the chromospheric Mg II emission (Fig. 6). The Linsky-Haisch boundary appeared to be "sharp" in the early IUE spectra for two reasons. First, the TR emission falls off rapidly with decreasing chromospheric activity levels, and the giants to the right of the dividing line generally have weak chromospheres. Second, the red giant ultraviolet spectra are dominated by chromospheric O I emission that is considerably enhanced relative to that of dwarf stars having comparable Mg II activity levels (Fig. 12). If one obtains low dispersion short wavelength spectra of dwarf and giant stars to optimally expose the brightest emission feature (aside from Lα), namely O I 1305 Å, then one would in effect be selectively underexposing at C IV in the giants compared with the dwarfs, by a factor of five or so. Since the IUE vidicons have a limited dynamic range, the factor of five in exposure can make the difference between "signal" and "noise" at C IV.

In short, the weakening of transition regions and coronae in the red giant branch is genuine, but appears "abrupt" primarily because of two selection effects: (1) The steep contrast between TR and Mg II emission; and (2) underexposures in the Lα region of giant stars driven by the selective enhancement of O I emission.

C. ON THE OCCURRENCE OF CHROMOSPHERES AND CORONAE IN LATE-TYPE STARS

The fact that coronal and TR emission are well-correlated with Mg II flux levels, at least in the cool stars for which all three have been detected,

suggests to me that chromospheres and coronae must be physically associated. However, the steepness of the soft X-ray correlation, and to some extent also that of the TR emission, suggests to me that the chromospheric and coronal heating mechanisms are quite different. The latter notion is strengthened by the discordant behavior of the F-stars in TR emission, and by the K giants and G-K supergiants in soft X-rays. The F-stars appear to support rather prominent TRs and coronae (e.g. Vaiana 1980), but comparatively weak chromospheres, while the cool giants and supergiants appear to be deficient in coronal material compared with dwarf stars of similar chromospheric Mg II emission.

I will now outline a speculative picture to tie together these disparate notions.

The detailed studies of the Sun during the Skylab era have strongly implicated magnetic fields as the fundamental building block in the solar outer atmosphere (Vaiana and Rosner 1978). The fields are responsible for the physical structuring of the coronal plasma and likely also for the heating.

If the solar corona and TR are heated by a magnetic agency, is it not reasonable that the chromosphere might be similarly heated, especially given the close correspondence of chromospheric brightness with mean magnetic field strength (Skumanich et al. 1975)? Actually, the answer is probably no, for the following reasons. The thermal energy density in the corona is much smaller than the magnetic energy density, consequently the dissipation of only a small fraction of the available coronal field, by reconnection for example, is required to balance coronal energy losses by radiation and backconduction to the chromosphere. On the other hand, the thermal energy density in the chromosphere is more nearly comparable to that of the magnetic field, consequently large volumes of field would have to be converted to heat on short timescales in order to power the large radiative losses in Mg II h and k and maintain the chromospheric temperature inversion.

An intriguing alternative to an in situ field dissipation mechanism for heating the chromosphere, is if the small-scale magnetic flux tubes thought to exist in the photosphere (Chapman 1980) serve simply as conduits of acoustic wave energy into the outer atmosphere. Magnetic flux tubes could, in principle, operate as acoustic wave guides owing to the reduced radiative damping of acoustic modes that results from the decreased gas pressures inside the tubes. (The gas pressures are lower owing to the large internal magnetic pressures.) Since the wave damping is proportional to the square of the gas pressure while the wave flux is directly proportional to the pressure, a potentially much larger absolute flux of wave energy could survive photospheric passage inside the tubes than in the unmagnetized plasma surrounding the tubes. In this picture, stellar chromospheres and coronae would be confined entirely to the interiors of magnetic flux tubes, but the heating mechanism in the distinct atmospheric layers would be quite different. Consequently, chromospheric and coronal emission levels should be grossly correlated, because the different atmospheric layers are physically associated through the agency of the magnetic field, yet the correlation need not have unit slope because the heat deposition mechanisms are distinct.

In this scenario, the weakening of chromospheres toward the early F stars is explained by a decrease in the acoustic wave flux as the stellar outer envelope becomes less convective. However, the TR and corona need not weaken correspondingly, since they are powered by the magnetic field directly. In particular, the rapid rotation of the F stars likely compensates somewhat for the reduced convective motions in the dynamo replenishment of surface fields. Alternatively, the F star chromospheres may be systematically thinner than those of cool stars owing to the enhanced photoionization of neutral hydrogen in the outer atmosphere by Balmer continuum radiation. The photoionization effect would strongly decouple the n_e/n_H ratio from its intrinsic temperature sensitivity, thereby removing the ionization "safety-valve" for the plasma cooling function that may be responsible for the extraordinary thickness (in pressure) of chromospheres in cooler stars.

The existence of the "corona-wind" boundary in the HR diagram is also understandable in the acoustic/magnetic scenario: A quirk of nature has allowed stars with very different main sequence heritages to evolve into nearly the same region of the HR diagram (Ayres 1980). Figure 13 depicts the phenomenon.

The heavy dashed curve represents the corona-wind boundary proposed by Linsky and Haisch. Evolutionary tracks for $1M_\odot$ (right-hand track) and $3M_\odot$ stars connect the Zero Age Main Sequence and the giant branch. Also included are contours of constant stellar radius, and arrows that indicate the general flow of stellar evolution in the two major regions which feed stars into the giant branch. Simple consideration of stellar statistics suggests that most of the comparatively numerous K giants must have evolved from main sequence stars only slightly more massive than the Sun. On the other hand, the less numerous G giants must evolve typically from $\cong 3M_\odot$ A-type or B-type stars. Consequently, the K giants tend to be old ($\gtrsim 10^9$ yr) and have evolved vertically in the HR diagram from relatively slowly rotating progenitors (F-G dwarfs). On the other hand, the G giants tend to be young ($\lesssim 10^8$ yr), and have evolved more nearly along the lines of constant radius from rapidly rotating progenitors (B-A dwarfs).

The substantial evolutionary expansion, advanced age, and slow-rotating predecessors of the K giants virtually guarantee that they too will be slow rotators. (In fact, the development of a massive chromospheric wind would rapidly shed any vestige of rotational angular momentum that had survived to that evolutionary stage.) Similarly, the modest evolutionary expansion and rapid-rotating precedessors of the youthful G giants virtually guarantee that they will be fast rotators (certainly compared with the K giants). The apparent weakening of chromospheric and coronal emission in the red giant branch, is then simply an artifact of comparing young magnetically active stars having vigorous dynamos to the left of the boundary with old, magnetically dying stars to the right. Chromospheres are considerably more visible in the K giants than are coronae, because the major component of the chromospheric heating, namely acoustic waves, is still active, despite the decay of the surface magnetic fields which are the sole coronal energy source.

The case of the supergiants is somewhat different from that of the giants. The supergiants have evolved horizontally in the HR diagram from very massive ($\gtrsim 10 M_\odot$) progenitors and must be quite young (10^6-10^7 yr). These stars have suffered enormous evolutionary expansion and are likely slow rotators as a result. Dynamo action must be comparatively weak in the supergiants once they have cooled sufficiently to develop convective envelopes. Nevertheless, because such stars are so young, one would anticipate that some of the primordial fields from the protostellar collapse would have survived dissipative processes over the relatively brief main sequence lifetime of the massive progenitor, and would therefore be available during the supergiant phase to form chromospheres and coronae by the scenario I have outlined above. Since the corona is a field-dissipative mechanism itself, and since the dynamo replenishment action is likely to be nil, one would expect to find a general weakening of the mean coronal emission levels with increasing age (toward cooler spectral types), and a peaking of chromospheric emission toward the early G supergiants where the rising acoustic flux production encounters the failing mean surface magnetic field levels.

D. CONCLUSION

I can only hope that the insight and impetus that the first and second years of IUE have given to the study of cool-star outer atmospheres will continue unabated into the third and future years.

REFERENCES

Athay, R. G. 1976, The Solar Chromosphere and Corona: Quiet Sun, (Boston: D. Reidel).

Athay, R. G. and White, O. R. 1978, Ap. J., 226, 1135.

_____. 1979, Ap. J. Suppl., 39, 333.

Avrett, E. H., Vernazza, J. E. and Linsky, J. L. 1976, Ap. J. (Letters), 207, L199.

Ayres, T. R. 1975, Ap. J., 201, 799.

_____. 1979, Ap. J., 228, 509.

_____. 1980, in Proceedings of "Cool Stars, Stellar Systems and the Sun," ed. A. K. Dupree, SAO Special Report, in press.

Ayres, T. R. and Linsky, J. L. 1980a, Ap. J., 235, 76.

_____. 1980b, Ap. J. (in press).

Ayres, T. R., Linsky, J. L. and Shine, R. A. 1975, Ap. J. (Letters), 195, L121.

Ayres, T. R., Marstad, N. and Linsky, J. L. 1980, in preparation.

Baliunas, S. L., Avrett, E. H., Hartmann, L. W. and Dupree, A. K. 1979, Ap. J. (Letters), 233, L129.

Baliunas, S. L. and Butler, S. E. 1980, Ap. J. (in press).

Basri, G. S. 1979, Ph.D. Thesis, Univ. of Colorado, Boulder, Colorado.

Basri, G. S. and Linsky, J. L. 1980, Ap. J., 234, 1023.

Basri, G. S., Linsky, J. L., Bartoe, J.-D. F., Brueckner, G. E. and Van Hoosier, M. E. 1979, Ap. J., 230, 924.

Bohm, H. U. 1980, preprint.

Böhm-Vitense, E. 1980a, preprint.

_____. 1980b, in Stellar Turbulence, eds. D. F. Gray and J. L. Linsky (New York: Springer-Verlag), p. 300.
Böhm-Vitense, E. and Dettmann, T. 1980, Ap. J., 236, 560.
Bopp, B. W. and Fekel, F., Jr. 1977, A. J., 82, 490.
Bruner, E. C., Jr. 1978, Ap. J., 226, 1140.
Cash, W., Bowyer, S., Charles, P., Lampton, M., Garmire, G. and Riegler, G. 1978, Ap. J. (Letters), 223, L21.
Chapman, G. A. 1980, in Proceedings "Skylab Series C Workshop: Active Regions," ed. F. Q. Orrall, (in press).
Cram, L. E., Krikorian, R. and Jefferies, J. T. 1979, Astr. Ap., 71, 14.
Doschek, G. A., Feldman, U., Bhatia, A. K. and Mason, H. E. 1978b, Ap. J., 226, 1129.
Doschek, G. A., Feldman, U., Mariska, J. T. and Linsky, J. L. 1978a, Ap. J. (Letters), 226, L35.
Dupree, A. K. 1975, Ap. J. (Letters), 200, L27.
_____. 1976, in Physique des mouvements dans les atmospheres stellaires, ed. Cayrel and Steinberg (Paris: CNRS), p. 439.
Dupree, A. K., Baliunas, S. L. and Shipman, H. 1977, Ap. J., 218, 361.
Dupree, A. K. and Hartmann, L. 1980, in Stellar Turbulence, eds. D. F. Gray and J. L. Linsky (New York: Springer-Verlag), p. 279.
Durney, B. R. 1972, The Solar Wind, NASA Report, ed. Sonett, Coleman and Wilcox.
Engvold, O. and Rygh, B. O. 1978, Astr. Ap., 70, 399.
Flannery, B. P. and Ayres, T. R. 1978, Ap. J., 221, 175.
Foukal, P. V., Huber, M. C. E., Noyes, R. W., Reeves, E. M., Schmahl, E. J., Timothy, J. G., Vernazza, J. E. and Withbroe, G. L. 1974, Ap. J. (Letters), 193, L143.
Golub, L., Harnden, F. R., Rosner, R., Topka, K. and Vaiana, G. S. 1980, B.A.A.S., 11, 775.
Hall, D. S. 1976, in Multiple Periodic Variable Stars, ed. W. S. Fitch (Dordrecht: D. Reidel), p. 287.
_____. 1978, A. J., 83, 1469.
Haisch, B. M. and Linsky, J. L. 1976, Ap. J. (Letters), 205, L39.
Haisch, B. M., Linsky, J. L. and Basri, G. S. 1980, Ap. J., 235, 519.
Haisch, B. M., Linsky, J. L., Weinstein, A. and Shine, R. A. 1977, Ap. J., 214, 785.
Hartmann, L., Dupree, A. K. and Raymond, J. C. 1980, Ap. J. (Letters) (in press).
Holt, S. S., White, N. E., Becker, R. H., Boldt, E. A., Mushotzky, R. F., Serlemitsos, P. J. and Smith, B. W. 1979, Ap. J. (Letters), 234, L65.
Hummer, D. G. and Stewart, J. C. 1966, Ap. J., 146, 290.
Iben, I., Jr. 1965, Ap. J., 142, 1447.
_____. 1967, Ann. Rev. Astr. Ap., 5, 571.
Kohl, J. H. 1977, Ap. J., 211, 958.
Linsky, J. L. 1980, in Proceedings Jan. 1980 HEAO-AAS Meeting (in press).
Linsky, J. L. and Ayres, T. R. 1978, Ap. J., 220, 619.
Linsky, J. L. and Haisch, B. M. 1978, Ap. J. (Letters), 229, L27.
Linsky, J. L., Worden, S. P., McClintock, W. and Robertson, R. M. 1979, Ap. J. Suppl., 41, 47.
Lites, B. W., Hansen, E. R. and Shine, R. A. 1980, Ap. J., 236, 280.
Lutz, T. E. 1970, A. J., 75, 1007.
Lutz, T. E. and Pagel, B. E. J. 1979, preprint.

Lutz, T. E., Furenlid, I. and Lutz, J. H. 1973, Ap. J., 184, 787.
Mariska, J. T., Doschek, G. A. and Feldman, U. 1980, Ap. J. (Letters) (in press).
McClintock, W., Henry, R. C., Moos, H. W. and Linsky, J. L. 1975, Ap. J. 202, 733.
Moos, H. W., Linsky, J. L., Henry, R. C. and McClintock, W. 1974, Ap. J. (Letters), 188, L93.
Mount, G. H., Rottman, G. and Timothy, J. G. 1980, preprint.
Noyes, R. W. 1974, contribution to IAU Symposium No. 27, Cambridge, Mass.
Nugent, J. and Garmire, G. 1978, Ap. J. (Letters), 226, L83.
Pagel, B. E. J. and Wilkins, D. R. 1979, preprint.
Parker, E. N. 1955, Ap. J., 122, 293.
_____. 1970, Ann. Rev. Astr. Ap., 8, 1.
Raymond, J. C. and Dupree, A. K. 1978, Ap. J., 222, 379.
Rosner, R., Tucker, W. H. and Vaiana, G. S. 1978, Ap. J., 220, 643.
Schmitz, F. and Ulmschneider, P. 1980, Astr. Ap. (in press).
Shine, R. A. and Linsky, J. L. 1972, Solar Phys., 25, 357.
_____. 1974, Solar Phys., 39, 49.
Skumanich, A. 1972, Ap. J., 171, 565.
Skumanich, A., Smythe, C. and Frazier, E. N. 1975, Ap. J., 200, 747.
Stencel, R. E. and Mullan, D. J. 1980, Ap. J. (in press).
Stencel, R. E., Mullan, D. J., Linsky, J. L., Basri, G. S. and Worden S. P. 1980, Ap. J. (in press).
Thomas, R. N. 1973, Astr. Ap., 29, 297.
Tripp, D. A., Athay, R. G. and Peterson, V. L. 1978, Ap. J., 220, 314.
Ulmschneider, P., Schmitz, F., Renzini, A., Cacciari, C., Kalkofen, W. and Kurucz, R. L. 1977, Astr. Ap., 61, 515.
Vaiana, G. S. 1980, in Proceedings Jan. 1980 HEAO-AAS Meeting (in press).
Vaiana, G. S. and Rosner, R. 1978, Ann. Rev. Astr. Ap., 16, 393.
Vaiana, G. S., et al. 1980, preprint.
Vernazza, J. E., Avrett, E. H. and Loeser, R. 1976, Ap. J. Suppl., 30, 1.
Walter, F. M., Cash, W., Charles, P. A. and Bowyer, C. S. 1980, Ap. J., 236, 212.
Walter, F. M., Charles, P. A. and Bowyer, C. S. 1978, A. J., 83, 1539.
Weiler, E. J. and Oegerle, W. R. 1979, Ap. J. Suppl., 39, 537.
Wilson, O. C. and Bappu, M. K. V. 1957, Ap. J., 125, 661.
Withbroe, G. L. 1977, in Proceedings of the OSO-8 Workshop (Boulder: University of Colorado Press), p. 2.
Withbroe, G. L. and Noyes, R. W. 1977, Ann. Rev. Astr. Ap., 15, 363.
Young, A. and Koniges, A. 1977, Ap. J., 211, 836.
Zahn, J. P. 1977, Astr. Ap., 57, 383.
Zwaan, C. 1980, in Proceedings, "Cool Stars, Stellar Systems and The Sun," ed. A. K. Dupree, SAO Special Report (in press).

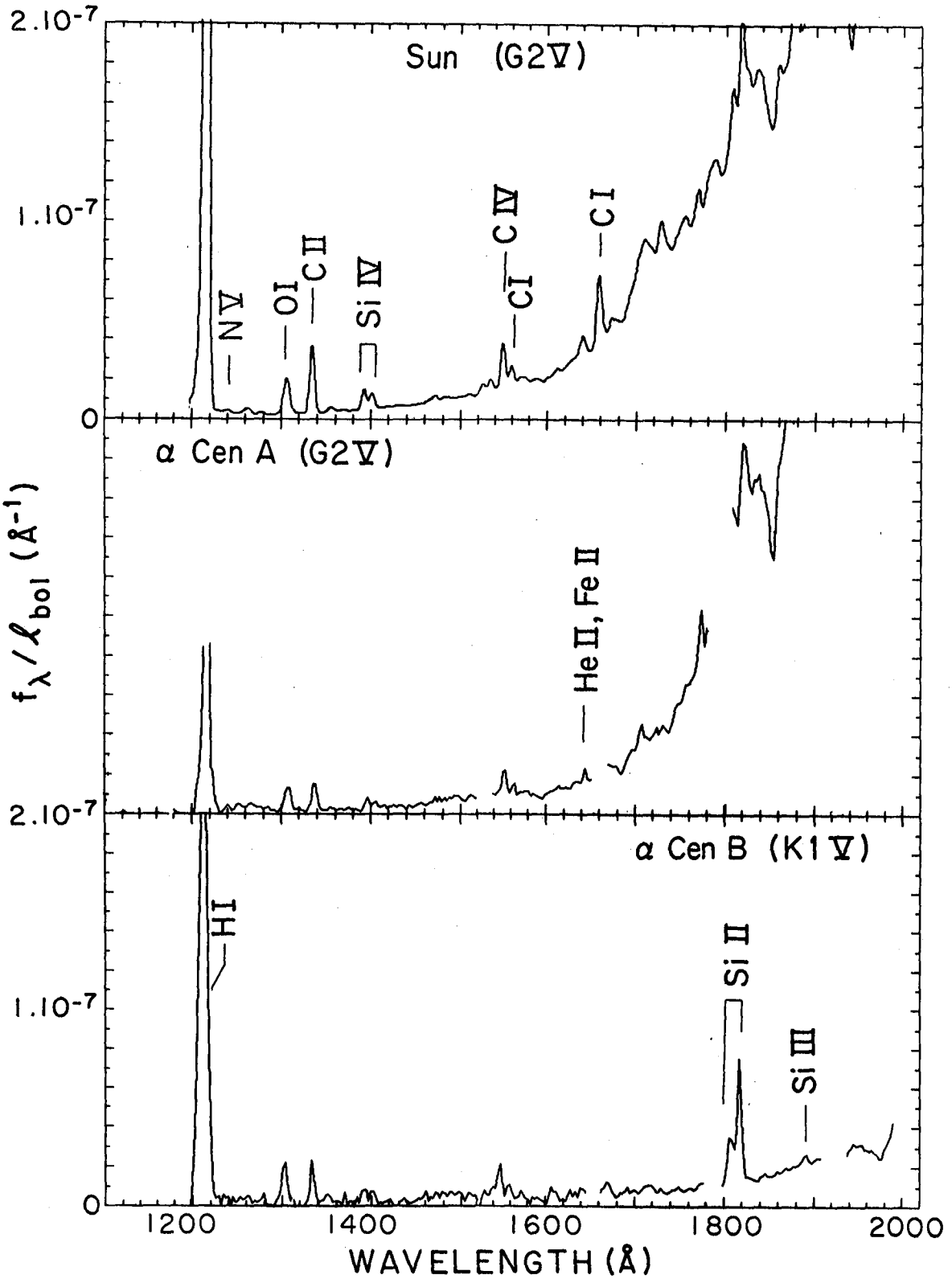

Fig. 1. Short wavelength, low dispersion IUE ultraviolet spectra of α Centauri A and B compared with the solar spectrum (as IUE would see it). Gaps in the stellar spectra are regions affected by saturation or reseau marks.

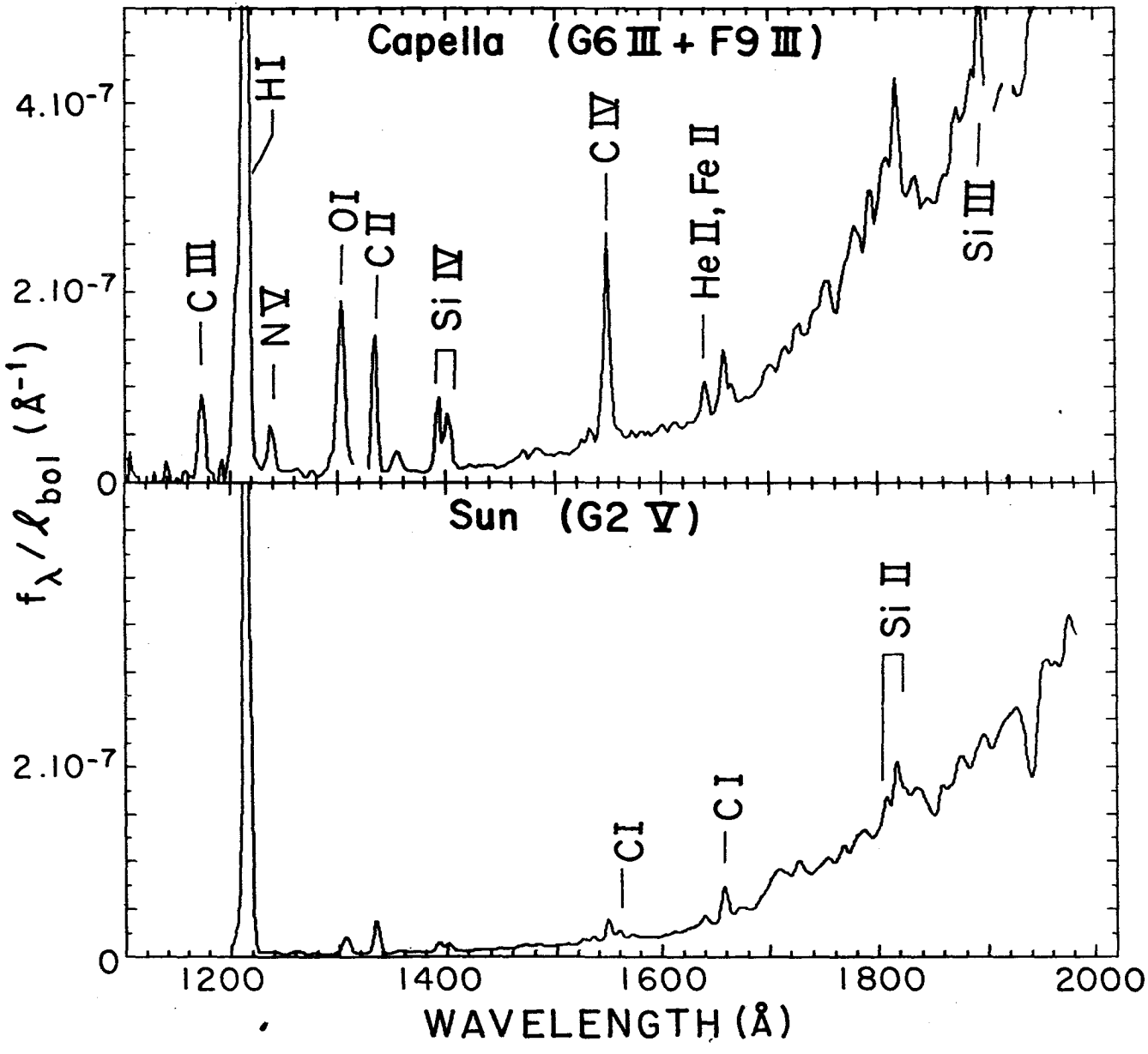

Fig. 2. Same as Figure 1 for Capella.

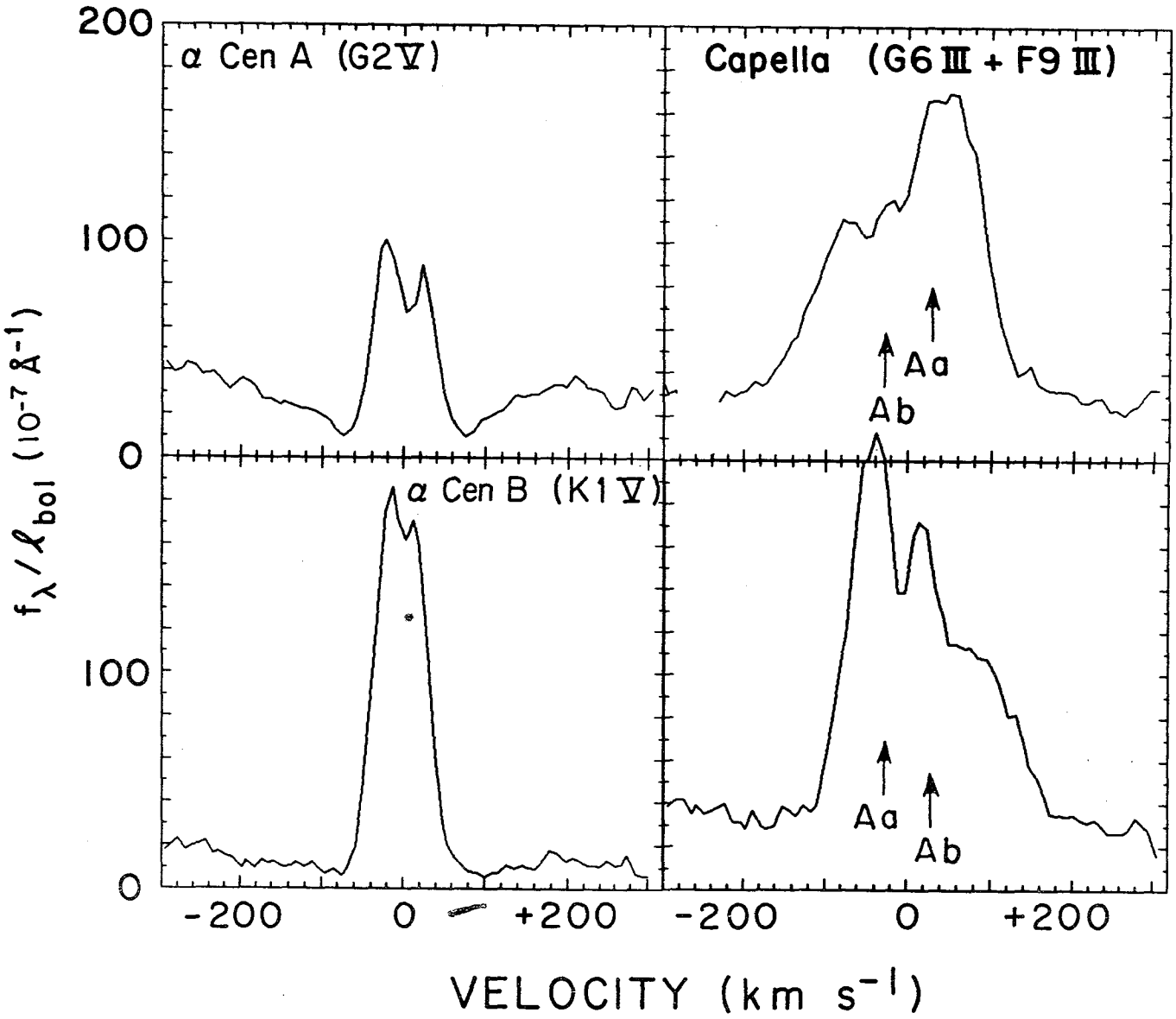

Fig. 3. LWR echelle-mode profiles of Mg II k (2796 Å) in α Centauri A and B, and Capella (orbital phase 26^d, top panel; phase 81^d, bottom panel).

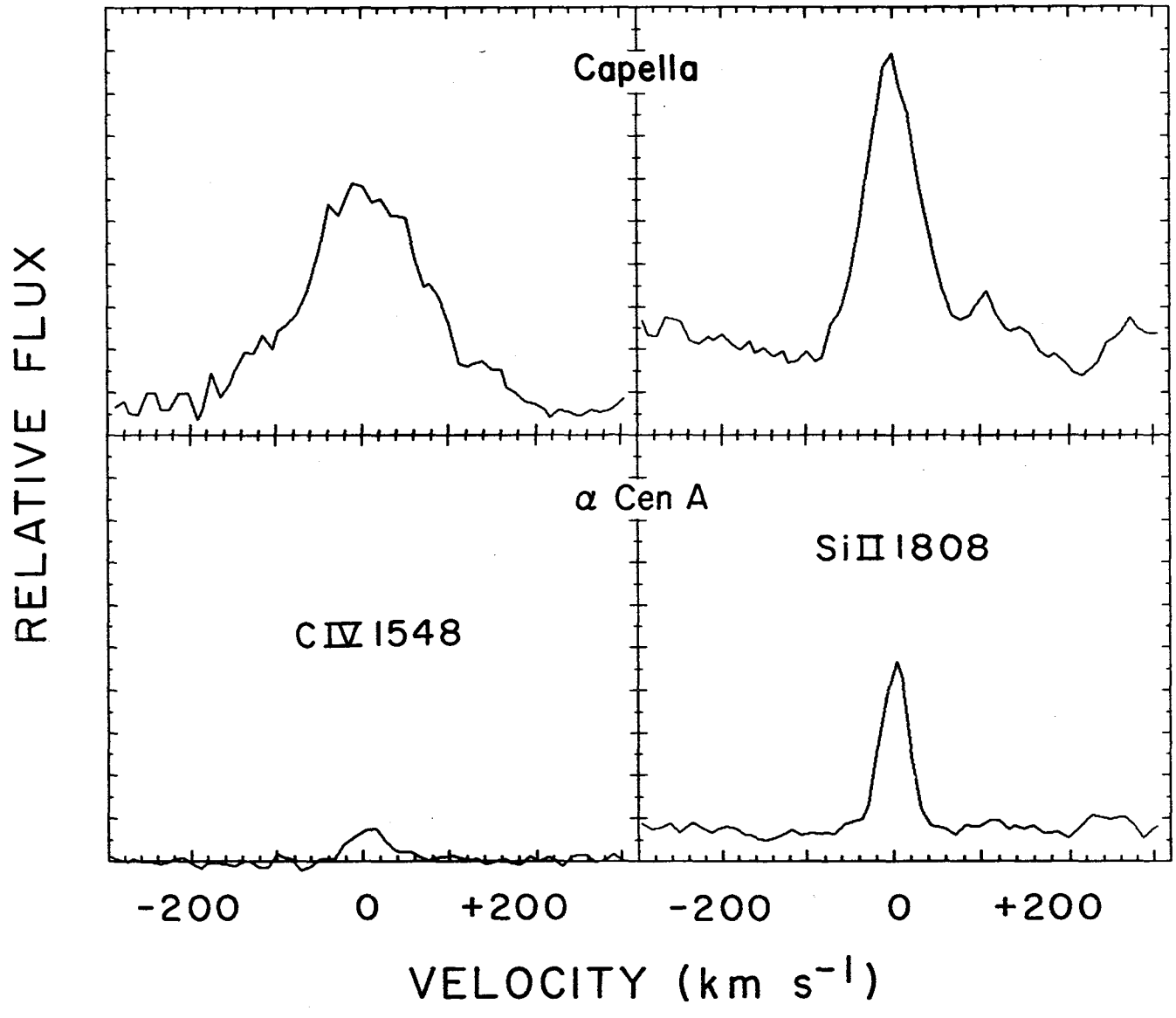

Fig. 4. Comparison of SWP echelle-mode profiles of C IV 1548 Å and Si II 1808 Å in α Centauri A and Capella.

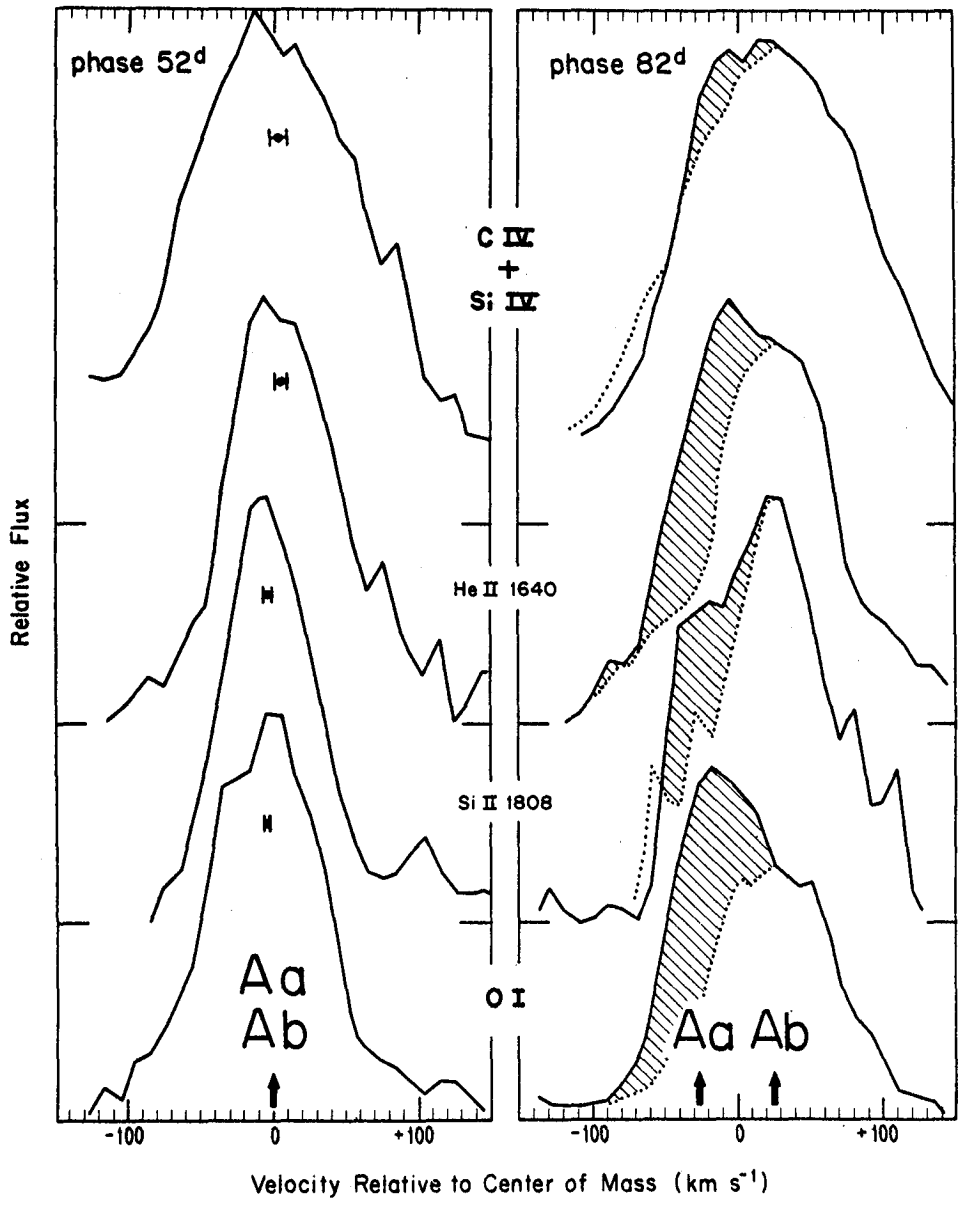

Fig. 5. Comparison of Capella chromospheric and transition region line profiles at two orbital phases: velocity crossing, left-hand panel; near elongation, right-hand panel. The COM velocities of the G-type primary (Aa) and F-type secondary (Ab) at each phase are indicated by arrows. (Courtesy Astrophysical Journal.)

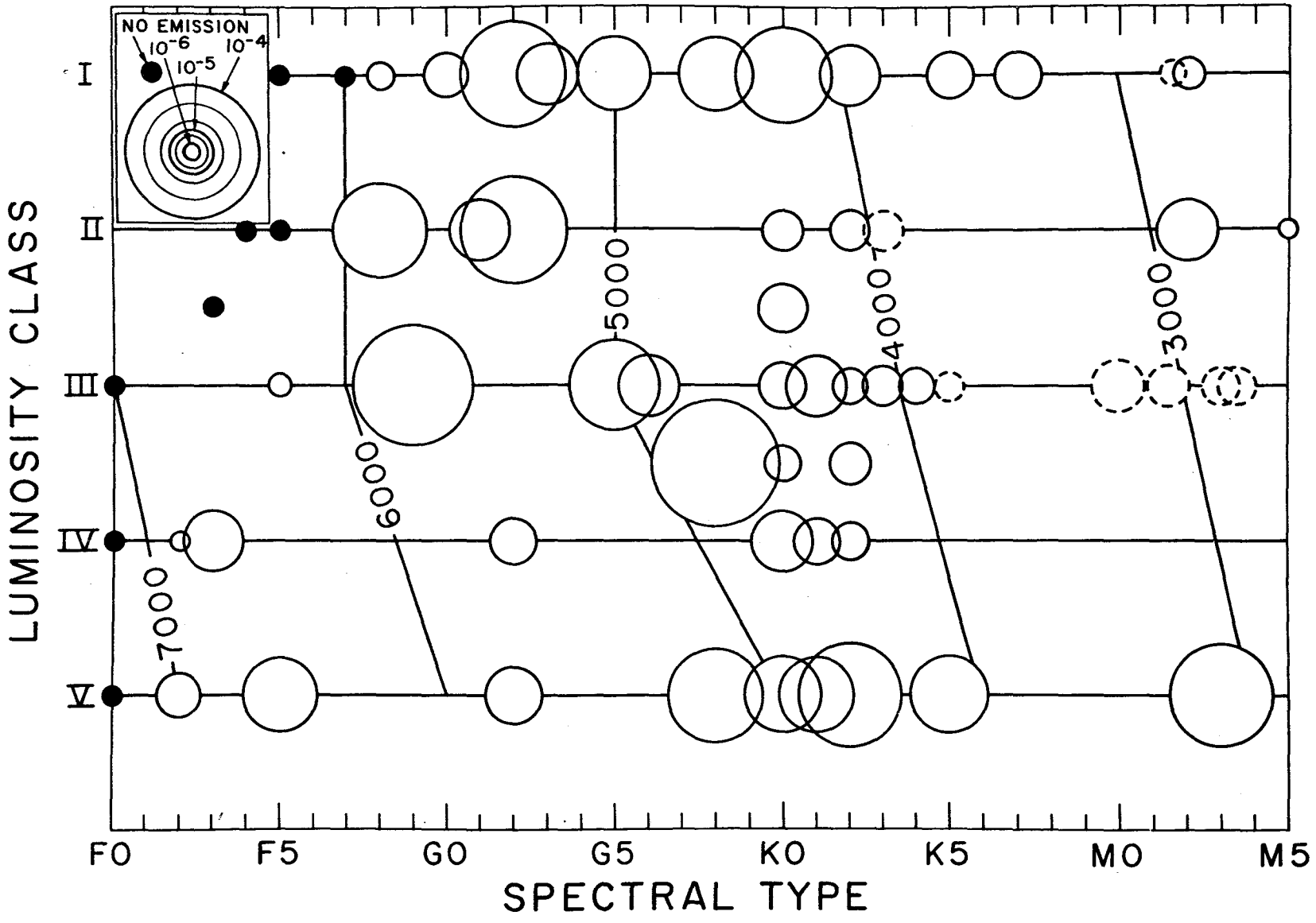

Fig. 6. Bubblegram of chromospheric radiative losses in Mg II h and k. Area of each bubble is proportional to the average value of $f_{\text{Mg II}}/\ell_{\text{bol}}$ in the particular spectral-type/luminosity-class bin. See legend, upper left-hand corner.

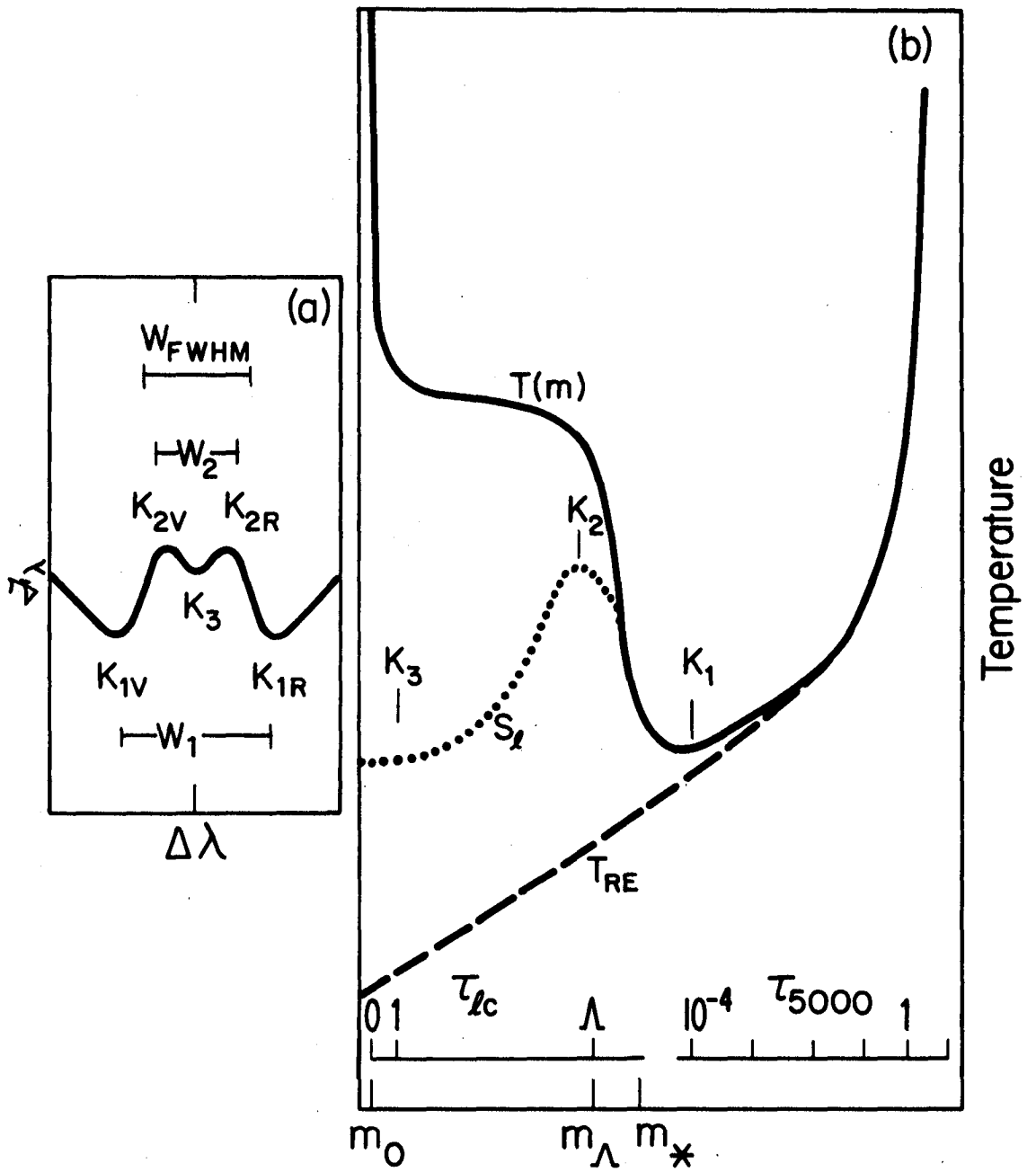

Fig. 7. Correspondence of atmospheric thermal structure (right-hand panel) to emission structure in Mg II k or Ca II K line profile. For example, the minimum temperature region at the top of the photosphere is mapped onto an intensity minimum in the line profile ("K_1"). The displacement of K_1 from line center is governed by the depth of the temperature minimum in mass column density, m_* (g cm^{-2}). If m_* increases, so does $\Delta\lambda_{K_1}$. (Courtesy Astrophysical Journal.)

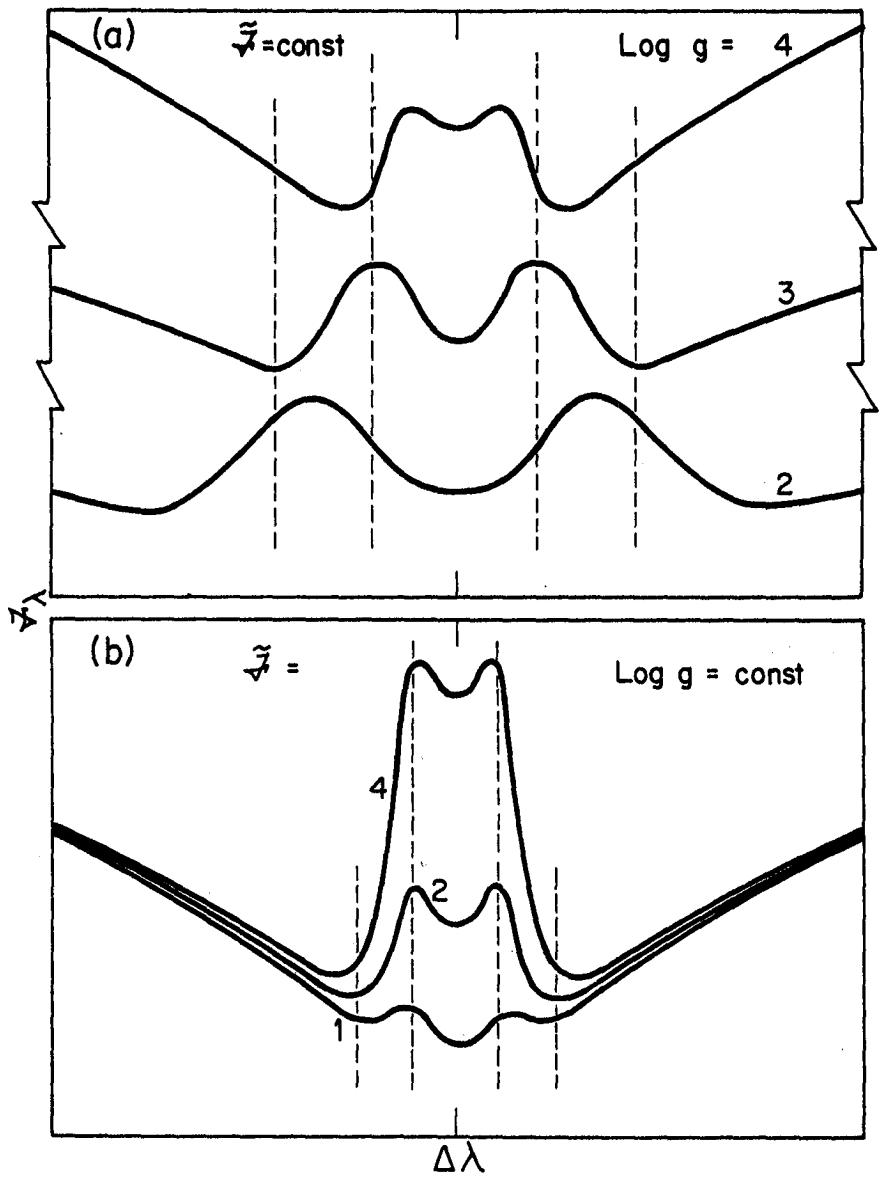

Fig. 8. Schematic depiction of Ca II K and Mg II k profile behavior with changing surface gravity (top panel) and chromospheric activity (bottom panel) as predicted by scaling laws. The intensity scale in the top panel is arbitrary for each profile. In particular, all three emission features should have similar integrated core surface fluxes. Note that the K_1 minimum feature separation broadens both with decreasing surface gravity and increasing chromospheric activity, while the K_2 separation broadens with decreasing surface gravity but becomes narrower with increasing activity. (Courtesy Astrophysical Journal.)

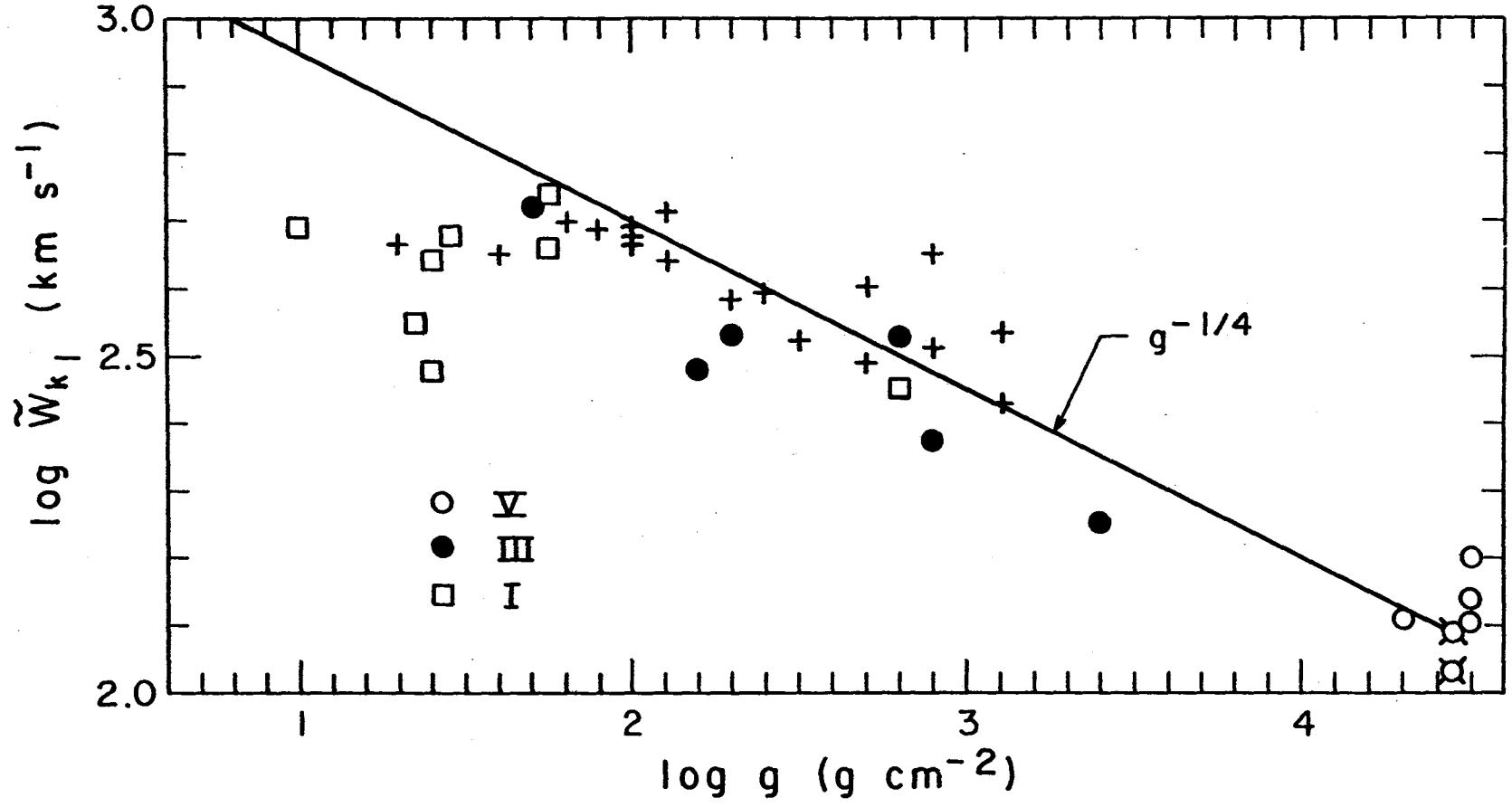

Fig. 9. Comparison of adjusted k_1 widths (see text) with estimated surface gravities. The $g^{-1/4}$ relation predicted by the scaling laws is illustrated by the solid curve that passes through the quiet Sun point.

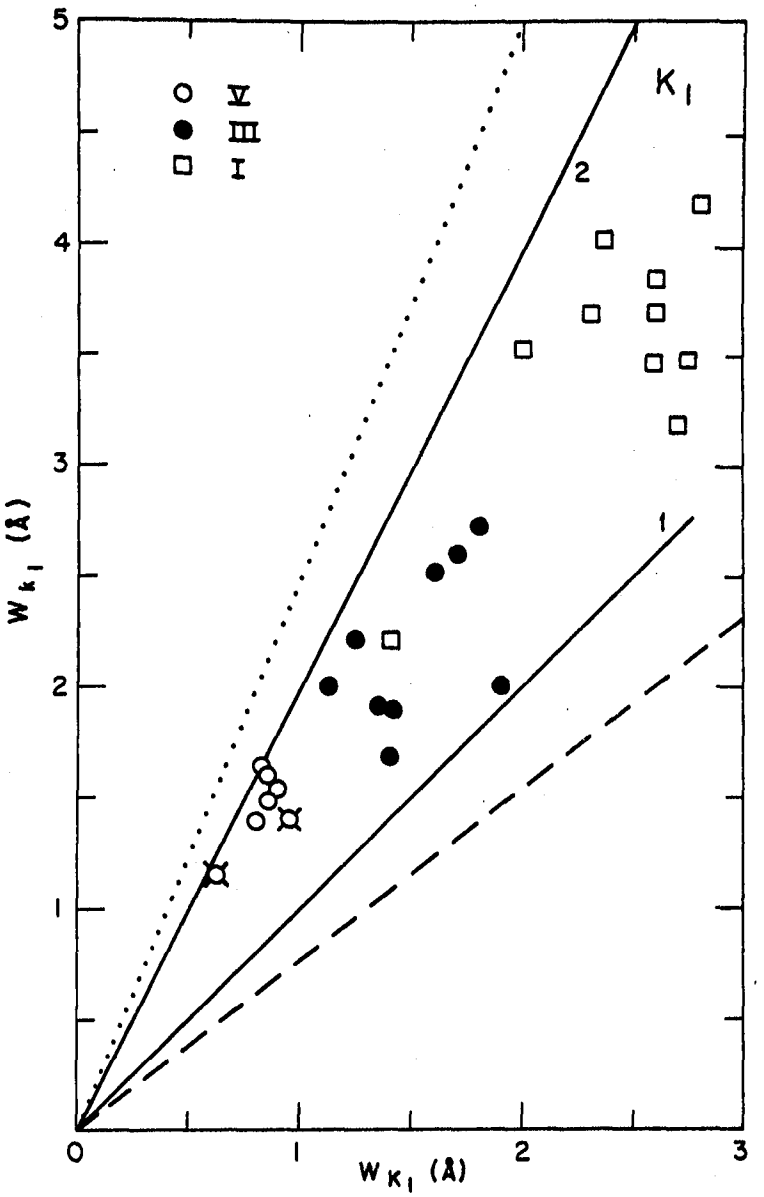

Fig. 10. Comparison of Mg II k_1 and Ca II K_1 separations for the available sample of dwarfs, giants and supergiants. The dotted curve depicts the 2.5 relation expected from the chromospheric scaling laws and "Damping" hypothesis, while the dashed curve is the relation expected if the minimum features were formed entirely in the Doppler core. Partial coherent scattering effects, which were not considered explicitly in the derivation of the scaling laws, would tend to reduce the 2.5 prediction somewhat. The decrease would be largest for the supergiants where the PCS effects are most pronounced.

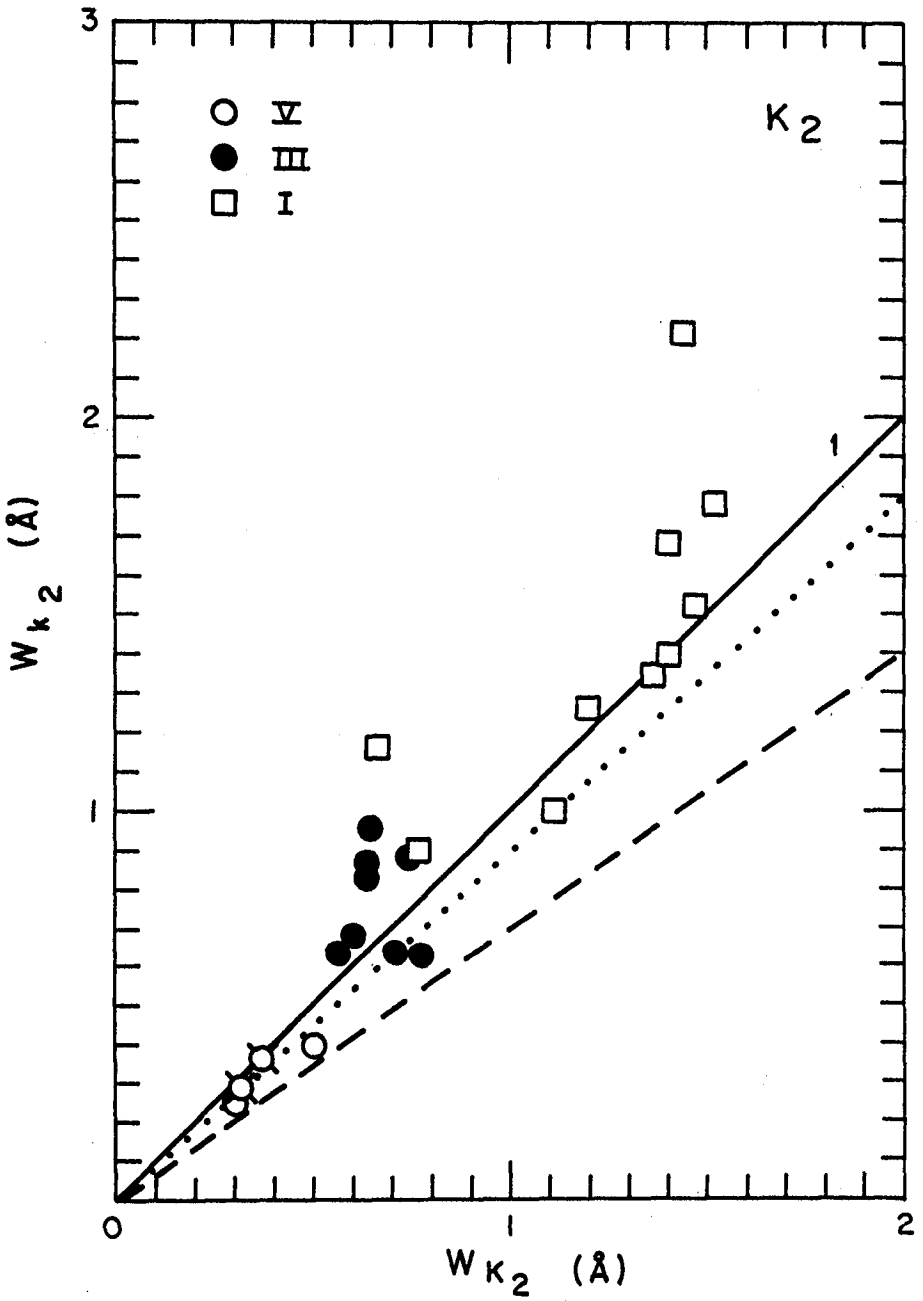

Fig. 11. Same as Figure 10 but for the k_2 and K_2 peak separation. The Damping (dotted curve) and Doppler (dashed curve) predictions are based on a depth-independent chromospheric broadening velocity. Both predictions would be increased if the nonthermal broadening in the middle chromosphere rises outwards. In addition, some of the measured k_2 widths may be overestimates of the true separations owing to the influence of interstellar and circumstellar absorption components in the k emission core.

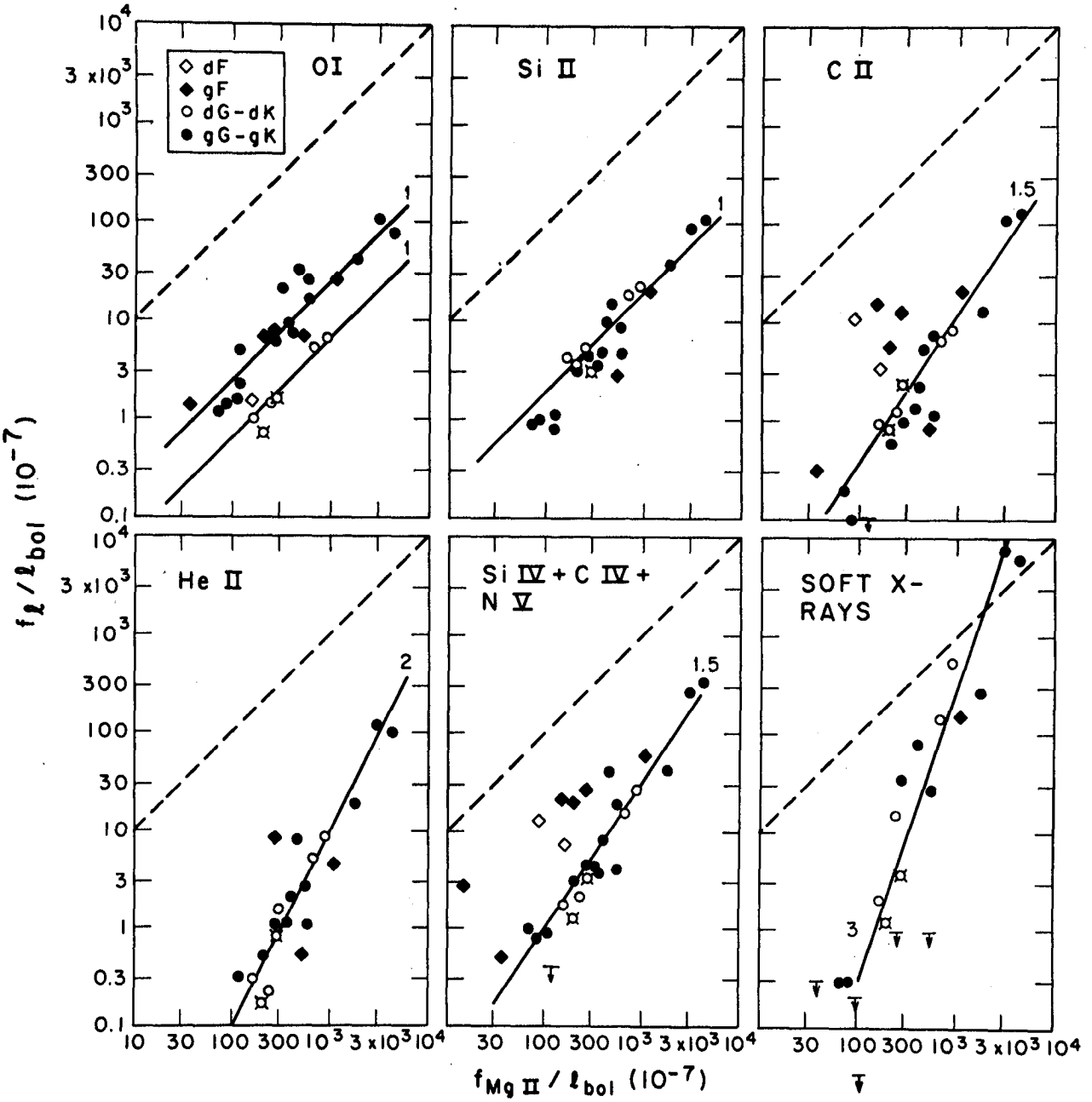

Fig. 12. Correlogram for chromospheric, transition region and coronal emission. The individual normalized fluxes are plotted against the normalized Mg II emission strength. The dashed curves in each panel are for $f_\ell / \ell_{bol} \equiv f_{Mg\ II} / \ell_{bol}$. Note that the Mg II emission is always considerably larger than that of the prominent features of the short wavelength spectrum. The solid curves are not fits to the data, but merely indicate the approximate slope of the individual correlations. (Courtesy Astrophysical Journal.)

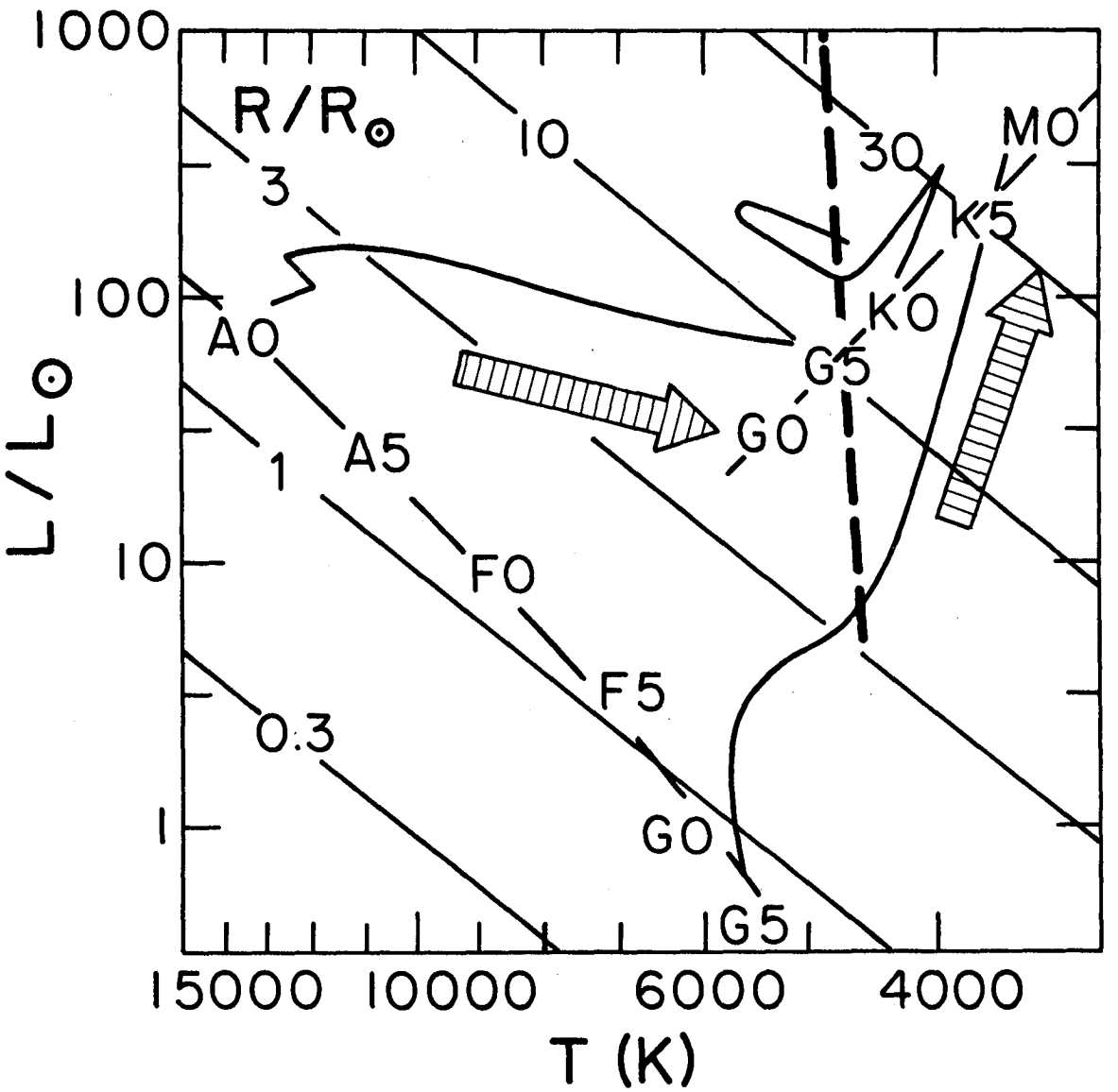

Fig. 13. A simple evolutionary scenario to explain the weakening of coronae and chromospheres, in the red giant branch. The heavy dashed curve is the corona-wind boundary proposed by Linsky and Haisch. The thin curves are evolutionary tracks (Iben 1967) for 1 $M_\odot$ (right-hand track) and 3 $M_\odot$ stars. The arrows indicate the general flow of evolution into the G and K giant regions. Spectral types are given for the Zero Age Main Sequence and in the yellow (F-G) and red (K-M) giant branches.